

APPLIED COMPUTER SCIENCE

The Journal is a peer-reviewed, international, multidisciplinary journal covering a broad spectrum of topics of computer application in production engineering, technology, management and economy.

The main purpose of Applied Computer Science is to publish the results of cutting-edge research advancing the concepts, theories and implementation of novel solutions in computer technology. Papers presenting original research results related to applications of computer technology in production engineering, management, economy and technology are welcomed.

We welcome original papers written in English. The Journal also publishes technical briefs, discussions of previously published papers, book reviews, and editorials. Especially we welcome papers which deals with the problem of computer applications in such areas as:

- manufacturing,
- engineering,
- technology,
- designing,
- organization,
- management,
- economics,
- innovations,
- competitiveness,
- quality and costs.

The Journal is published quarterly and is indexed in: BazTech, Cabell's Directory, CNKI Scholar (China National Knowledge Infrastructure), ERIH PLUS, Index Copernicus, J-Gate, Google Scholar, TEMA Technik und Management.

Letters to the Editor-in-Chief or Editorial Secretary are highly encouraged.

CONTENTS

Dariusz PLINTA, Martin KRAJČOVIČ APPLICATION OF THE AUGMENTED REALITY IN PRODUCTION PRACTICE.....	5
Lukasz DZIAK, Malgorzata PLECHAWSKA-WOJCIK THE USE OF UNITY 3D IN A SERIOUS GAME DEDICATED TO DEVELOPMENT OF FIREARM HANDLING SKILLS.....	15
Łukasz WOŹNIAK, Paweł SURDACKI, Leszek JAROSZYŃSKI THE NUMERICAL MODEL OF 2G YBCO SUPERCONDUCTING TAPE IN THE WINDINGS OF THE TRANSFORMER.....	23
Konrad PIETRYKOWSKI, Tytus TULWIN THE NONUNIFORMITY OF THE PISTON MOTION OF THE RADIAL ENGINE.....	39
Svetlana RATNER, Pavel RATNER DEA-BASED DYNAMIC ASSESSMENT OF REGIONAL ENVIRONMENTAL EFFICIENCY.....	48
Kamil JONAK, Paweł KRUKOW MATCHING PURSUIT ALGORITHM IN ASSESSING THE STATE OF ROLLING BEARINGS.....	61
Sławomir KUKLA, Marek SMETANA A SIMULATION EXPERIMENT AND MULTI-CRITERIA ASSESSMENT OF MANUFACTURING PROCESS FLOW VARIANTS TESTED ON A COMPUTER MODEL.....	72
Marian JANCZAREK, Oleksij BULYANDRA COMPUTER AIDED THERMAL PROCESSES IN TECHNICAL SPACES.....	82

augmented reality, digital factory

Dariusz PLINTA^{}, Martin KRAJČOVIC^{**}*

APPLICATION OF THE AUGMENTED REALITY IN PRODUCTION PRACTICE

Abstract

Current requirements which are connected with designing new, or realizing the existing production systems, cause continuous and rapid changes in products and processes. This means that classical approaches of production systems design have to be extended by advanced technologies and methods, such as digital factory, virtual and augmented reality, computer simulation, reverse engineering, etc. The article describes new computer technologies, which were applied in production practice, with a particular focus on the augmented reality technology.

1. INTRODUCTION

The contemporary global market requires from producers quick realization of orders, low cost and high quality of products. These requirements create the need for collaboration of all professions from engineers and managers to shop floor workers, and sharing knowledge and experience (Brzeziński, 2007; Gregor, Medvecký, Mičieta, Matuszek & Hřčková, 2007). Nowadays competitive environment requires utilization of new software systems for design, testing, process planning, manufacturing and assembly. Application of such a digital framework for production allows to achieve higher quality, flexibility, quickness and efficiency. The use of new concepts of computer-aided manufacturing and process planning can be done simultaneously with product design, shortening time of production and working towards lean manufacturing practice. Such an approach allows for quick identification of potential problems and elimination of their negative consequences for the organization.

^{*} University of Bielsko-Biala, Production Engineering Department, Willowa 2, 43-309 Bielsko-Biala, +48 33 8279 234, dplinta@ath.bielsko.pl

^{**} University of Žilina, Industrial Engineering Department, Univerzitná 1, 010 26 Žilina, Slovak Republic, + 421 41 513 2718, martin.krajcovic@fstroj.uniza.sk

2. AUGMENTED REALITY

Augmented Reality (AR) is one of the fastest growing part of virtual reality. The basis of augmented reality is the ability to combine elements of the real and virtual worlds into a single view (Azuma, 1997; Haas, 2004; Westkaemper, Bischoff, Von Biel & Duerr, 2001). Augmented reality is a technology supported by human visual perception. The combination of real and virtual objects makes possible to transfer to the user a variety of additional information. The condition of this technology is to preserve the link with the user and real environment. In the virtual reality we create a model of a real production system, which can be used as a model for augmented reality. In the second mentioned technology (AR) we do not replace all the real world, but only the selected virtual elements corresponding to objects from the analysed real environment. The view can be realized using a monitor and a camera or with a head mounted display (Bajana, 2013). In practice, we can use two types of augmented reality systems:

1. Systems using position sensors and transparent display. The position sensor sends information about the position and direction of the user. Basing on this information, the scene generator prepares for display virtual objects located in the user's area of vision and projected on semi-transparent mirror through which the user sees the real scene.
2. Capturing real camera image for the registration of markers which indicate virtual objects position. A video camera captures the real scene and sends it to the computer. The software on the computer is looking for markers, calculates the camera position and distances between markers and assigns them to marker image of the virtual object and then displays the resulting image of the real scene with virtual objects.

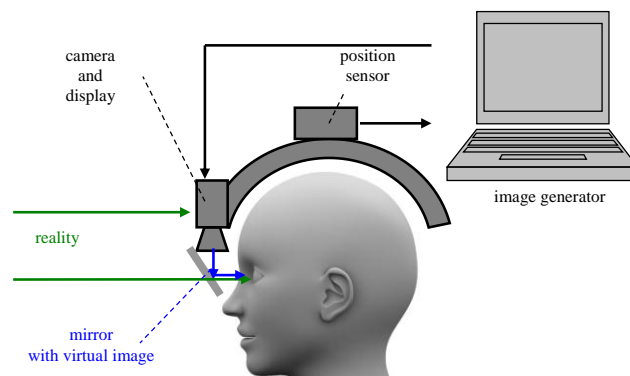


Fig. 1. Basic principles of augmented reality systems

3. CREATION OF A REAL PRODUCTION SYSTEM IN VIRTUAL REALITY ENVIRONMENT

A virtual model of a real production system can be created using various CAD programs, or using special applications dedicated to this purpose, such as CeitTable (Furmann & Krajčovič, 2009).

A production system model generally can be created in the following steps:

1. Preparation of 2D/3D objects:
 - a) Usage of libraries of 2D/3D objects from the applied software. Current objects of the library can be further complemented and expanded by new own objects.
 - b) Acquiring new 3D models using reverse engineering methods and 3D laser scanning technology, DMU (Digital Mock Up) and FMU (Mock Up Factory) models.
 - c) Creating new models using CAD applications.
2. Modelling of the production system:
 - a) Defining the production area.
 - b) Copying objects from the library to the created production model.
 - c) Defining transport relations between objects.
3. Layout optimization:
 - a) Sankey diagram.
 - b) Intensity-Distance diagram.
 - c) calculation the overall transport performance.
 - d) triangular method.
 - e) safety work analysis.
4. Visualization of the production system:

2D or 3D layout of the production system, which is presented by computer monitor, or using virtual technology and augmented reality.

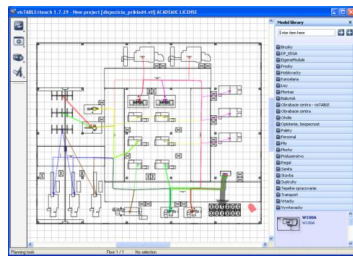
The creation of a virtual model of a real system requires the following activities:

1. Replacement of dimensionless workplaces by objects with real shapes and dimensions of machines/workplaces,
2. Placing in the created model a required number and particular types of machines/workplaces according to the results of capacity calculations.

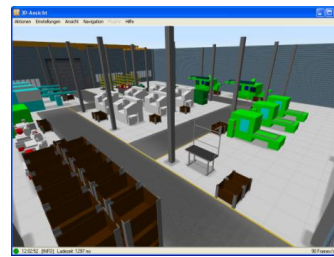
At the beginning of the modelling process we should prepare earlier mock-ups of machines and workplaces and create the first (ideal) arrangement. This initial deployment will be supplemented by transport links between machines visualized by the material flow diagram (Fig. 2a).

Additionally, we should take into account:

- a) service areas of workplaces,
- b) material flow in the production hall and between halls,
- c) needs of transportation and material handling,
- d) building structures and media installations.



a) 2D model



b) 3D model

Fig. 2. Virtual models of production systems (Plinta & Krajčovič, 2015)

The result of the described work is a realistic virtual model of workplaces or production halls, which respects all the existing constraints in production presented in a 2D or 3D view (Fig. 2).

4. PRODUCTION SYSTEMS VISUALIZATION WITH AUGMENTED REALITY

At universities in Bielsko-Biala and Zilina, we are currently developing the concept of Digital Factory with progressive approaches to visualization of digital information (Furmann & Krajčovič, 2009; Gregor, Plinta, Furman & Štefánik, 2011; Plinta & Krajčovič, 2015; Štefánik & Furmann, 2011). It seems appropriate to apply augmented reality (AR – Augmented Reality) technologies for designing and visualization of production systems (Bajana, 2013).



Virtual reality – computer-modelled environment



Augmented Reality – a combination of the real environment and virtual objects

Fig. 3. The difference between the virtual and augmented reality (Plinta & Krajčovič, 2015)

Research on the use of AR in designing of production and logistics systems is currently focused on the application of augmented reality systems based on creation of a real scene and identification of tags (markers) in the camera recorded scenes, which define user position and orientation in the modelled scene (Gabajová, 2013; Gabajová, Krajčovič & Plinta, 2013; Mirandová & Gabaj, 2011).

The below example is related with the concept of interactive projection system created at the University in Zilina, which is based on the projection on the planning table. The current version of this system uses 3D visualization layout of the production system presented on a monitor screen or a wall using a data projector. It is a projection of the 3D model to a 2D view.

By using augmented reality in designing of production systems with the planning table, we can create extended visualization in which 3D models are placed directly on the planning table. 3D models emerge from the layout, what is presented in figure 4. Using markers placed on the production layout drawn on a planning table and 3D models of machines, it is not necessary to use any additional data projector displaying the designed production system.

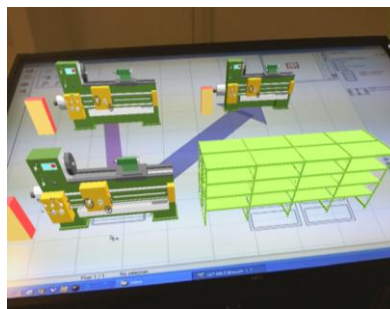


Fig. 4. Visualization using augmented reality technology on the planning table (Mirandová & Gabaj, 2011)

The proposed solution uses markers to identify the position and type of the 3D object, which are displayed above them, and also to determine the position and orientation of the user's viewpoint (camera) in the observed scene (the projection area of the table). The production system which is created with a planning table can be also presented by means of augmented reality in the real environment of the production hall. Showing virtual objects in a real environment, we can observe and analyse production systems for identifying possible organizational problems and evaluating the final position of particular workplaces in production halls. Using such tools, we can find possible collisions with other workplaces, walls, with power devices, machinery and equipment for power distribution, interconnection of production machinery and equipment with the current transportation and handling system, and potential problems with installing new machinery and equipment, etc.

5. AUGMENTED REALITY IN THE PICKING PROCESS

The picking process consists of several following steps (Fig. 5) (Krajčovič, 2011; Mirandová & Gabaj, 2011):

1. Identification of the worker – the worker is logged into the system and confirms his identity;
2. Identification of the picking contract – chosen from a list of specific contracts of the searched order;
3. Identification of the storage of each item – identifying the exact location of items and obtaining the storage coordinates in relation to a given reference point of the coordinate system;
4. Proposal for order picking items and determining routes beats – on the basis of the list of items, a list of collecting items is created from the first to the last, according to the principles of finding them, for example with the shortest path;
5. Realization of the picking process – the process of collecting items;
6. Registration of the picked material – update of the residual inventory of selected items.

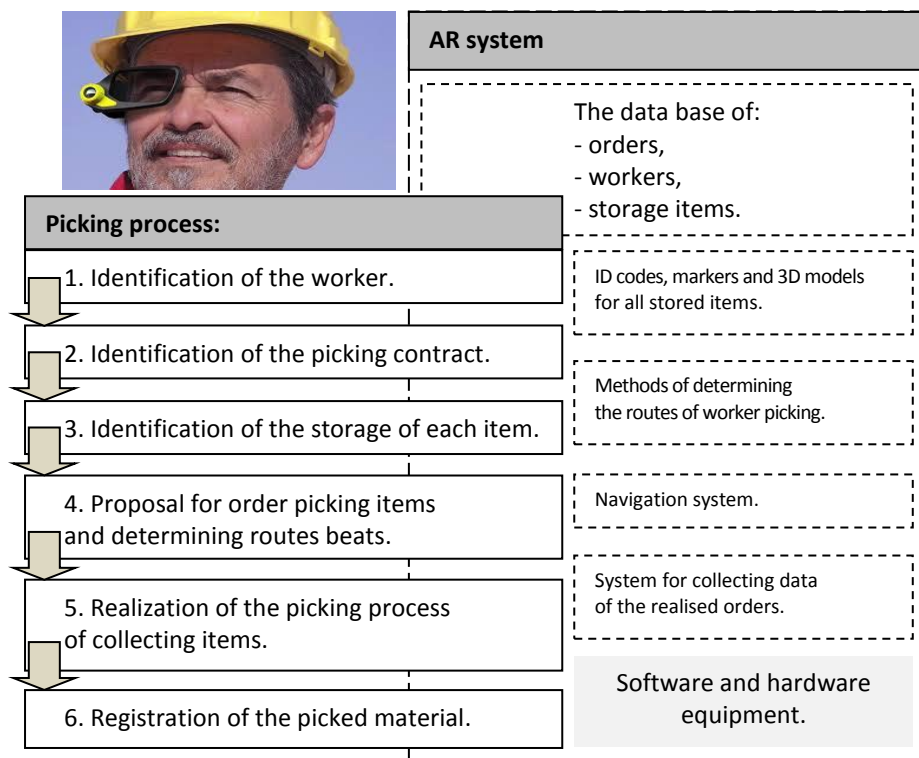


Fig. 5. Picking process with AR

Generally, the process of picking using augmented reality is connected with additional activities, like:

1. Extracting information about orders and stored items from WMS.
2. Extracting information about ID code of markers for all ordered items.
3. Determining location and selection of navigation markers to determine the directional navigation.
4. Generating information for navigation in the store.
5. Preparing glasses for augmented reality and booting the system.
6. Using technical means of augmented reality trip between picking locations.
7. Collecting data about the realised orders.

Integration of the augmented reality technology into the picking process gives us a possibility of eliminating the most common mistakes in picking items from the stores.



Fig. 6. Picking items with augmented reality (Mirandová & Gabaj, 2011)

6. AUGMENTED REALITY IN ERGONOMICS

Augmented Reality and Virtual Reality may appear to be effective solutions for complex analyses of developed designs of prototype workplaces, according to requirements of work safety and ergonomics in the following areas:

- management of health and safety,
- manual weight lifting,
- work with computer monitors,
- use of personal protection,
- use of machines and tools,
- design of workplaces.

A workplace designed in an appropriate manner allows the operator to work in the most effective way possible. In the time of rapid changes in demand it is necessary to flexibly react to customer requirements. Because of that it is necessary to rebuilt and change the existing working and assembly workstations to improve the working process, and especially working conditions.

An example of ergonomic analysis using virtual reality created in ErgoMax is presented in figure 7.

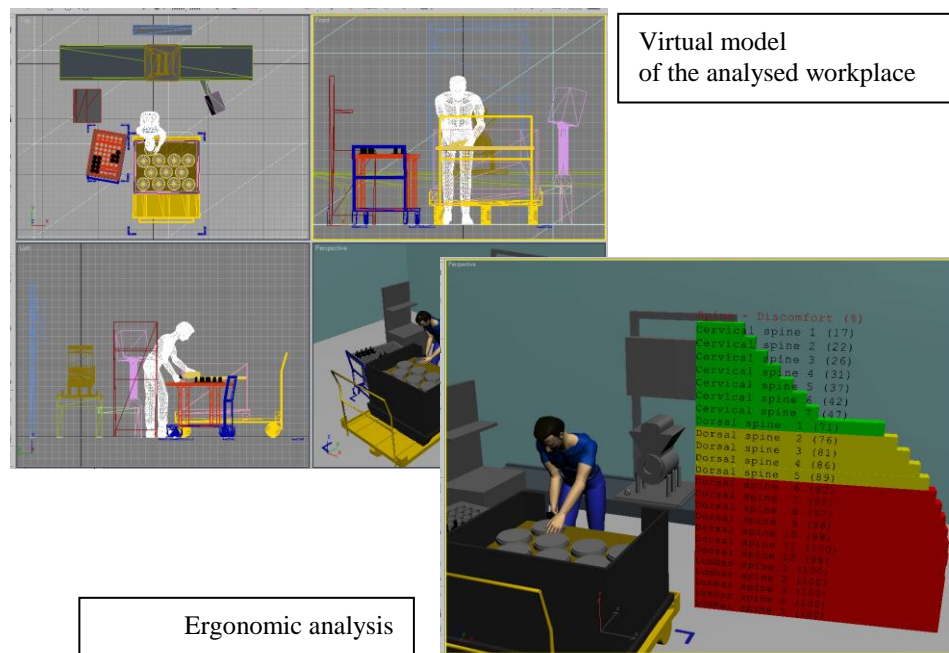


Fig.7. Ergonomic analysis using virtual reality (source: own study)

Virtual workplace is a system consisting of an appropriate VR hardware and software. Stages of VR application in analysis of workplaces include:

1. CAD model transfer to VR application and improvement of 3D object appearance by applying visualization techniques, such as texture mapping, lighting effects, reflections etc.
2. Programming objects' behaviour – movement as a response to a user-generated event (mouse click, keyboard button press, entering the defined collision zone) or an event generated by another object.
3. Creating user interface – the interface must be intuitive and allow easy launching of all the necessary functions of the virtual model.
4. Application testing – verification of the analysed workplace and their possible improvements.
5. Application in practice – finished application may be used in the process of education of future operators of the workplace, which will shorten the time needed to introduce an operator to work on the new workplace with full efficiency and safety.

Modern information technologies give us a range of possibilities to test new ways of working and to design and evaluate workplaces. Such analyses can be conducted with different software, like for example Delmia, Tecnomatix and features in the CAVE environment. These technologies are constantly being developed for new practical applications. They will be very helpful as the current versions already shorten time of designing workplaces, ergonomic analysis and significantly reduce costs (Dulina & Smutná, 2010; Januszka, 2012).

7. CONCLUSIONS

The rapid development of computer technologies and advanced software solutions support the designing process and allow for testing different things in a virtual environment. This gives us a possibility to save expenses for prototyping and implementing corrective actions caused by wrong decisions which appear during the designing stage. Extending modern technology usage to almost all areas of business activity has led to the definition of the digital factory concept.

The contribution shows a possibility of linking traditional approaches and methods of production design and organization of production processes (preparation and analysis of input data, the use of optimization algorithms) with new technologies of digital data processing (virtual reality and augmented reality technology) and methodology for designing and visualizing production systems.

REFERENCES

- Azuma, R.T. (1997). A Survey of Augmented Reality. *Teleoperators and Virtual Environments*, 6, 355–385.
- Bajana, J. (2013). Innovative presentation of information using augmented reality. In L. Dulina (Ed.), *Advanced Industrial Engineering* (pp. 155-170). Bielsko-Biala: FCNT.
- Brzeziński, M. (2007). *Wprowadzenie do nauki o przedsiębiorstwie*. Warszawa: Difin.
- Dulina, L., & Smutná, M. (2010). *Methods and software support in industrial ergonomics*. Zilina: Slovenská ergonomická spoločnosť (SES).
- Furmann, R., & Krajčovič, M. (2009). Interactive 3D Design of Production Systems. In *Digital Factory 2009 – Workshop Handbook*. Zilina: SLCP.
- Gabajová, G. (2013). Picking process using augmented reality. In L. Dulina (Ed.), *Advanced Industrial Engineering* (pp. 41–66). Bielsko-Biala: FCNT.
- Gabajová, G., Krajčovič, M., & Plinta, D. (2013). Navigation with augmented reality. In *InvEnt 2013 – modern technologies - way to higher productivity*. Zilina: University of Zilina, EDIS.
- Gregor, M., Medvecký, Š., Mičieta, B., Matuszek, J., & Hřčeková, A. (2007). *Digital Factory*. Zilina: KRUPA print.
- Gregor, M., Plinta, D., Furman, R., & Štefáňik, A. (2011). Digital factory – 3d laser scanning, modelling and simulation of production processes. In J. Matuszek, M. Gregor, & B. Mičieta (Eds.), *Metody i techniki zarządzania w inżynierii produkcji* (pp.39-50). Bielsko-Biala: Wydawnictwo Akademii Techniczno-Humanistycznej.
- Haas, W. (2004). *AK-Digitale Fabrik. Bericht Roadmap*. Ingolstadt: Audi.
- Januszka, M. (2012). Projektowanie ergonomiczne z zastosowaniem technik poszerzonej rzeczywistości. In *XI Forum Inżynierskiego ProCax*, 2–4.10.2012.
- Krajčovič, M. (2011). Projektovanie výrobných dispozícií s podporou rozšírenej reality. In *Produktivita a inovácie* (pp. 27–29). Zilina: University of Zilina.
- Mirandová, G., & Gabaj, I. (2011). Use of augmented reality in storing and picking components from warehouse. In J. Matuszek, M. Gregor, & B. Mičieta (Eds.), *Metody i techniki zarządzania w inżynierii produkcji*. Bielsko-Biala: Wydawnictwo Akademii Techniczno-Humanistycznej.
- Plinta, D., & Krajčovič, M. (2015). Production systems designing with the use of digital factory and augmented reality technologies. In R. Szewczyk, C. Zieliński, & M. Kaliczyńska (Eds.), *Progress in automation, robotics and measuring techniques: control and automation* (pp. 187–196). Cham, Heidelberg: Springer.
- Štefáňik, A., & Furmann, R. (2011). Computer simulation – aided designing of production and logistics systems. In: *AI magazine - journal about the automotive industry, mechanical engineering and economics* (pp. 46–47).
- Westkaemper, E., Bischoff, J., Von Biel, R., & Duerr, M. (2001). Factory Digitalizing – An adapted approach to a digital factory planning in existing factories and buildings, *Werkstattstechnik*, 91.

serious games, educational games, firearm handling game

Lukasz DZIAK*, Malgorzata PLECHAWSKA-WÓJCIK*

THE USE OF UNITY 3D IN A SERIOUS GAME DEDICATED TO DEVELOPMENT OF FIREARM HANDLING SKILLS

Abstract

The paper presents the model of the serious game designed to develop firearm handling skills. The game is dedicated to act as an educational tool. Its aim is to teach how to disassembly and assembly weapons. The main aim of the paper is to present and discuss educational value of this kind of serious games. Detailed results were obtained after end user examination. What is more, the aspect of ergonomic and usability is also covered. The paper presents also the game design and development process.

1. INTRODUCTION

Serious games are currently very popular. Furthermore, this popularity is continuously rising. However foundations for serious games had been laid before computer games gained popularity. The term serious games in its current form was mentioned for the first time by Clark Abt in a book “Serious Games” (Abt, 1970). He defined serious games as games which have educational use instead of being used only for entertainment. There were some other important publications after that (Jansiewicz, 1973), but real popularity of the topic came with 21st century. Besides works like Michael’s and Chen’s (Michael & Chen, 2006) which tried to comprehensively discuss the serious game topic there were many articles and scientific papers focusing on one chosen area of this kind of games. Studies on serious games included education, medicine, military and many others. Treating depression might be one of the examples (Plechawska-Wójcik & Rybka, 2015; Weina, Gromala & Tong, 2015; Fleming et al., 2014).

* Institute of Computer Science, Lublin University of Technology, Nadbystrzycka 36B, Lublin, 20-618, Poland, +48 81 525 20 46, lukasz.dziak@pollub.edu.pl, m.plechawska@pollub.pl

There are also applications made for medicine purpose, for example for diabetic people (Diehl et al., 2015). Educational games could be successfully used in schools (Fisser, Voogt & Bom, 2013) and for employee skills development (Corrigan et al., 2015). They are used for military training as well. A good example is a French game which teaches combat casualty care (Pasquier et al., 2016). American army also uses games that teach battlefield behavior, as well as encourage future adepts to join the army (Alvarez & Michaud, 2008).

When it comes to research papers related directly with firearms handling skills there are also many positions available. Article “LVC interaction within a mixed-reality training system” (Pollock et al., 2012) presents foundations, usage and problems connected with development of battlefield simulator called Veldt. It mixes real elements like rooms, foyers and doors with virtual reality. It is made using video projectors, sensors and purpose-built weapons. Game Virtual Battlespace 2 is the main part of the system. The work is summarized by a survey conducted among system users. Thereby it was possible to distinct positives and negatives of the system and discuss possible improvements.

Quite similar but simpler simulation is presented and elaborated in another research work (Bhagat, Liou, & Chang, 2016). Presented game is made mainly for military shooting range simulation. Thanks to laser technology shots made using special weapons are transferred to virtual world with very high precision. The article is summed up by a survey conducted among high school students who played the game. According to the survey results both game reception and educational effects were positive.

Market research show that serious games connected with development of firearm handling skills focus mostly on shooting. It seems that there is a lack of games teaching how to disassembly and assembly firearms. It seems that this topic is not popular. This is one of the reasons why this paper addresses mentioned topic. Gun disassembly and assembly is one of the potential subjects that could undergone scientific research.

The aim of the paper is to present the gameplay of the serious game focusing on disassembly and assembly firearms and to evaluate educational value of this kind of games. The rest of the paper is structured as follows. The section 2 presents the idea of the game, the section 3 presents the details of the survey used for research. The section 4 presents obtained results. The section 5 concludes the work.

2. THE IDEA OF GUN DISASSEMBLY AND ASSEMBLY GAME

2.1. Game design

The aim of the presented game is to teach potential players partial assembly and disassembly of AKMS assault rifle. The target platform is personal computer with Windows operating system. The game consists of two main modes:

learning mode and time trial. The aim of the first mentioned mode is to teach a player how to assembly and disassembly weapon. It is realized in the form of step by step tutorial. The second mentioned mode is to polish up skills gained in previous mode. A player tries to achieve the best result. Achievements that could be collected in this mode give a player additional motivation. There are also statistics which allows a user to keep track of his/her progress. What is more, there is information about weapon used in game, so as to satisfy players curiosity when they search for detailed knowledge.

The learning mode is made in a tutorial like form. There are instructions shown on the screen telling a player which actions should be performed at the moment. There are also many tips. Gun parts connected with current game point are highlighted. Also labels with gun parts names are shown. Gameplay is divided into two stages: gun disassembly and gun assembly. Figure 1 presents sample actions performed by the user during gun disassembly. Underneath them there are messages displayed to a player.

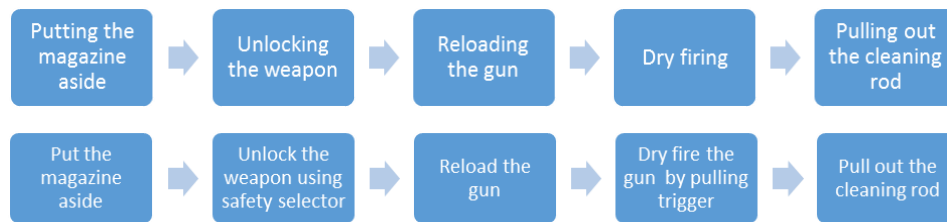


Fig. 1. Sample actions performed in the learning mode

The time trial is in many aspects quite similar to learning mode. One of the biggest differences is the lack of instructions in this mode. Moreover, both disassembly and assembly time are measured. The aim of this mode is to disassembly and assembly weapon in the shortest possible time. Player mistake results in a time penalty. Figure 2 shows mechanics of time trial game mode using BPMN schema.

2.2. Game implementation

The game was implemented using various tools. Gun model was created in Blender. In general game was made with use of Unity 3D development tools. C# was the language used in the process.

Making model was probably the most time consuming task during implementation phase. AKMS assault rifle model was made with great attention to details and with division to single gun parts. It was textured with accordance to reality.

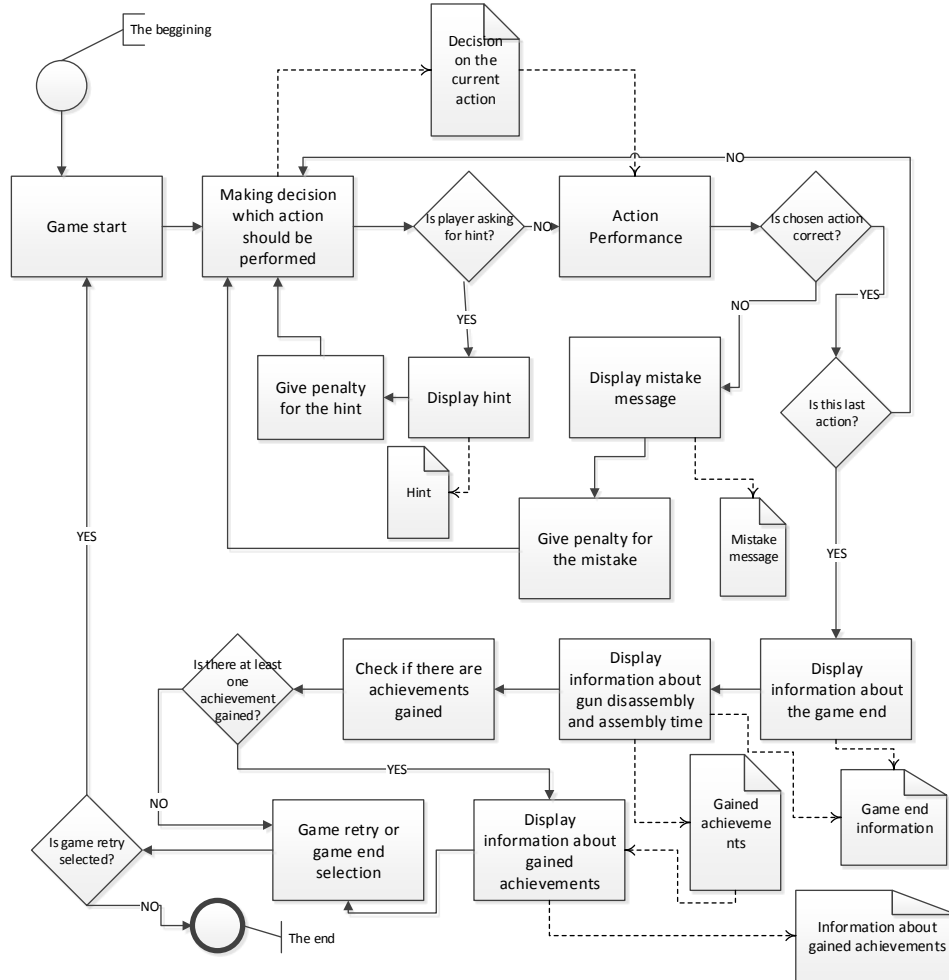


Fig. 2. The time trial BPMN schema

Animations are very important part of the game. All animations were defined using C# delegates. Third-party library called GoKit Tween was used to simplify and speed up animation development process.

There are achievements which player can gain for performing tasks well. Information about them is stored in an NoSQL database. The same is made for the statistics. One important thing to note is that gained statistics are used in achievement awarding process. Some of the statistics are shown to the player, so he/she can keep track on his/her game progress.

Hint system in the game consists of two parts: highlighting weapon elements and their name labels. Highlighting was made using custom shader. Highlighted weapon elements are visible even if they are behind other objects.

A special class was developed to show element name labels in appropriate places. It was used to translate 3D coordinates to 2D coordinates. Such operation was necessary because label hints (2D GUI elements) are to be shown where 3D elements are presented.

Final step of the implementation process was game balancing. Like in any other computer game it was necessary to properly adjust difficulty level. Animations duration was changed in order to match reality. Achievements were redesigned in order to give a player more motivation. It was hard and time consuming process, as it consisted of many retests of the game. Figure 3 shows the screenshot of the game learning mode.



Fig. 3. Learning mode screenshot

3. THE SURVEY

A special survey was conducted in order to examine educational value of the game as well as its usability features. Before filling the questionnaire respondents had to play the game at least 30 minutes in total. They had to spend at least 15 minutes in the learning mode and the same amount of time in the time trial. Questions about educational values of the game were divided into three groups: questions checking gained knowledge, questions related to playing time, questions about subjective game effects estimation. The first group included five questions asking about things like weapon elements assembly order or elements used in the disassembly process. Its aim was to check in an unbiased manner what players have learned. The second group consisted of questions about time spent both in the learning mode and in the time trial. The third group asked respondents about their own opinion about game and effects of playing it. Usability examination was made in order to check how GUI design affects the player experience.

People who took part in the research didn't have experience in disassembling or assembling AKMS rifle. They also had small or none firearm handling experience. It was checked in survey using special questions. The group consisted of 20 people. They were on average 25.6 years old, standard deviation of their age was 6.35 years and median was 24. Exactly 80% of the responders were man and 20% were women.

4. RESULTS OF SURVEY

Survey showed that the game is regarded as a good educational tool. Both verifying questions and responders subjective opinion show that game taught players how to disassembly and assembly guns. Maximum number of points which could be scored from questions checking gained knowledge was 5. On average interviewees scored 3.95 points, whereas standard deviation was 0.94 points and median 4 points.

70% of responders declared that after playing they are able to disassembly and assembly the gun presented in the game. 30% told that they could do it partially. In contrast, 85% of them declared that before playing the game they were totally unable to disassembly AKMS. Figure 4 shows comparison between ability to disassembly and assembly AKMS rifle before and after playing the game.

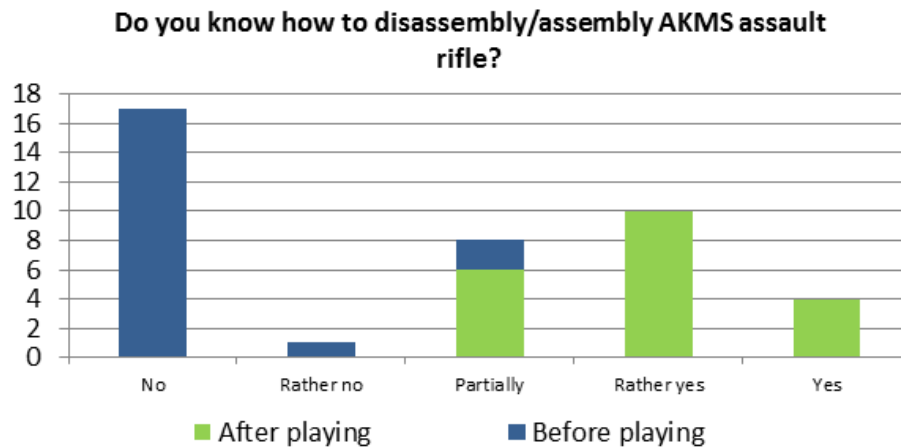


Fig. 4. Ability to disassembly/assembly rifle before and after playing the game

50% of the people declared that the game is very useful, whereas 45% told that it is useful. One person thinks that it is only partially useful. Those results shows that the game has very positive reception among interviewees.

Some questions were made to check whether game impacts people to get interested in guns and shooting. All of them had only two possible responses: “yes” or “no”. Results are as follows:

- All responders (100%) after playing the game declared that they would like to retry doing the same things in real life,
- 95% would play the game one more time if there were new guns added,
- 85% declared that the game encouraged them to go to a shooting range,
- Half of the responders (50%) admitted that they would like to search for additional information about firearms in external sources.

It could be easily seen that the game enhances players to take part in activities connected with firearms.

Usability examination showed good readability of the main menu. However, its appearance rating was slightly worse. It means that outlook of the main menu should be improved.

Further questions were about fonts size, contrast between elements and selection of colors. According to answers, font size is proper and contrast is quite good. Although colors should match better. Game elements like navigation, instructions placement and prompt readability are proper.

The biggest issue is that there are moments in which a player doesn’t know what to do next. What is more there are also situations where after clicking on some object there is no expected reaction. There should be further study performed on this matter. It is important to determine what is the reason of such opinions and improve the game afterwards.

5. CONCLUSIONS

The main goal of this paper was to present and discuss the results of examination of educational value of the serious game and its usability. Performed study shows that developed game meets users expectations. The game has high educational value. Responders surely developed firearms handling skills using it. Usability of the game is good, although there are elements which should be improved. Game itself might be used as an educational tool. Not only by individuals but also by institutions.

REFERENCES

- Abt, C. (1970). *Serious Games*. USA: Viking Press.
- Alvarez, J., & Michaud, L. (2008). *Serious Games: Advergaming, edugaming, training and more*. France: IDATE.
- Bhagat, K., Liou, W., & Chang, C. (2016). A cost-effective interactive 3D virtual reality system applied to military live firing training. *Virtual Reality*, 20 (2), 127–140.
- Corrigan, S., Zon, G., Maij, A., McDonald, N., & Mårtensson L. (2015). An approach to collaborative learning and the serious game development. *Cognition, Technology & Work Journal*, 17 (2), 269–278.
- Diehl, L., de Souza, R., Gordan, P., Esteves, R., & Coelho, I. (2015). Effectiveness of a serious game for medical education on insulin therapy for diabetes: randomized controlled trial. *Diabetology & Metabolic Syndrome Journal*, 7 (1), Supplement. doi:10.1186/1758-5996-7-S1-A163
- Fisser, P., Voogt, J., & Bom, M. (2013). Word Score: A serious vocabulary game for primary school underachievers. *Education and Information Technologies*, 18 (2), 165–178.
- Fleming, T., Cheek, C., Merry, S., Thabrew, H., Bridgman, H., Stasiak, K., Shepherd M., Perry, Y., & Hetrick S. (2014). Serious games for the treatment or prevention of depression: A systematic review. *Journal of Psychopathology and Clinical Psychology*, 19 (3), 227–242. doi: 10.5944/rppc.vol.19.num.3.2014.13904
- Jansiewicz, D. (1973). *The New Alexandria Simulation: A Serious Game of State and Local Politics*. USA: Canfield Press.
- Michael, D., & Chen, S. (2006). *Serious Games: Games That Educate, Train, and Inform*. Canada: Thomson Course Technology PTR.
- Pasquier, P., Mérat, S., Malgras, B., Petit, L., Queran X., Bay, C., Boutonnet, M., Jault, P., Ausset, S., Auroy, Y., Perez, J. P., Tesnière, A., Pons, F., & Mignon, A. (2016). A Serious Game for Massive Training and Assessment of French Soldiers Involved in Forward Combat Casualty Care (3D-SC1): Development and Deployment. *Journal of Medical Internet Research Serious Games (JMIR Serious Games)*, 4(1), 48–57. doi:10.2196/games.5340.
- Plechawska-Wójcik, M., & Rybka, J. (2015). A Serious Game Raising Awareness And Experience Of Depression. *The 9th International Technology, Education and Development Conference (INTED 2015)*, Spain, Madrid.
- Pollock, B., Winer, E., Gilbert, S., & de la Cruz, J. (2012). LVC interaction within a mixed-reality training system. *The Engineering Reality of Virtual Reality 2012*. USA Burlingame.
- Weina, J., Gromala, D., & Tong, X. (2015). Serious Game for Serious Disease: Diminishing Stigma of Depression via Game Experience. *Games Entertainment Media Conference (GEM)*. Canada, Toronto.

YBCO 2G tape, superconducting transformer, current limitation

Łukasz WOŹNIAK*, Paweł SURDACKI*, Leszek JAROSZYŃSKI*

THE NUMERICAL MODEL OF 2G YBCO SUPERCONDUCTING TAPE IN THE WINDINGS OF THE TRANSFORMER

Abstract

Computer assisted calculations consists in applying software for the simulation of models of certain devices and later analysing their behavior under given conditions corresponding to real working conditions in a specific environment. The paper proposes a circuit model of 2G YBCO superconducting tape created in the PSpice program. The model consists of passive blocks and active user blocks of analogue behavioural modelling (ABM). ABM blocks calculate the conductances, the currents of the individual layers of the superconducting tape, its thermal capacity, the heating power, the cooling power and resulting temperature of the tape. The model uses table of thermal power density passed to the liquid nitrogen vs. temperature. Smooth transition of the YBCO superconductor layer into the resistive state is described by Rhyner's power law. The developed model was used for generating waveforms of thermal and electrical quantities.

1. INTRODUCTION

Superconductors enable to combine magnetic and electrical properties of materials, which can be noticed thanks to the loss of electrical resistance and some peculiar magnetic phenomena under specific conditions. Superconductors are in the superconducting state when the working point determined by temperature, current density and magnetic field intensity is below the critical surface characteristic for each superconducting material.

* Lublin University of Technology, Institute of Electrical Engineering & Electrotechnologies, Nadbystrzycka 38A, 20-618 Lublin, e-mail: wozniak.lukasz1988@gmail.com, p.surdacki@pollub.pl, l.jaroszynski@pollub.pl

A general classification of superconductors is introduced due to the critical temperature value:

- LTS – Low Temperature Superconductor,
- HTS – High Temperature Superconductor.

The critical temperature $T_C = 25$ K is the point separating LTS and HTS superconductors (Tinkham, 2004).

2. YBCO 2G SUPERCONDUCTING TAPE

2.1. The structure of 2G YBCO superconducting tape

Second generation high temperature superconducting tapes (2G HTS) are called layered or coated conductors. These tapes are usually based on yttrium high-temperature superconductor YBCO. Second generation tapes begin to replace the tapes and wires of the first generation (1G HTS), which were based on bismuth superconductor BSCCO. Characteristic about the second generation tapes in superconducting state is that they conduct current of hundreds amperes at very low losses. Additionally, when the second generation superconductor obtains the resistive state, an unlaminated tape has a relatively high resistance.

High temperature superconducting tapes of second generation are made of several relatively thin layers. A base layer is responsible for electrical and mechanical parameters and in many cases consists of non-magnetic Hastelloy (Ni – 57,00%, Mo – 16,00%, Cr – 15,50%, Fe – 5,50%, W – 4,00%, Co – 2,50%). The thickness of this layer is about 50 μm (Table 1). An optional layer of stabilizer which determines the performance of thermal and also mechanic parameters of the tape, is located at the top and bottom of the tape and has the thickness of about 20 μm . 2G YBCO tape comprises a silver layer having thickness of about 2 μm , YBCO superconducting layer having thickness of about 1 μm , a buffer layer LaMnO_3 (LMO) having thickness of 30 nm, a homoepitaxial layer MgO having thickness of 30 nm and a base layer MgO having thickness of 10 nm. Tapes produced by American Superconductor (AMSC) are covered with laminate coating of stainless steel, copper or brass. In turn, SuperPower company produces tapes without a stabilizer (SF series) and tapes with copper stabilizer (SCS series). While comparing these two types of second generation superconducting tapes (Fig.1 and Fig.2), it can be predicted that tapes without a stabilizer show many times higher resistance than tapes with a stabilizer above the temperature T_C (Majka & Kozak, 2009; Tinkham, 2004).

Tab. 1. The parameters of SCS4050 superconducting tape by SuperPower (SuperPower Inc., 2016)

Type of tape	SCS 4050
Thickness	~ 0.1 mm
Width	4 mm
Minimum bending radius	25 mm
Critical current (at $T = 77$ K, self-field)	80-100 A
Maximum length of a single section of the tape	> 600 m
Thickness of Ag layer	2 μm
Thickness of Cu layer	40 μm
Thickness of YBCO layer	1 μm
Thickness of Hastelloy C276	50 μm
Resistivity of substrate	$1.24 \cdot 10^{-6} \Omega\text{m}$

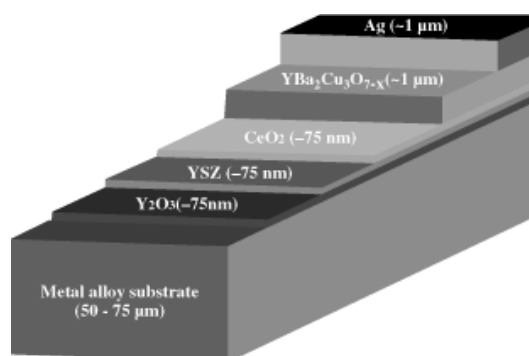


Fig. 1. The structure of second generation superconducting tape by AMSC (American Superconductor, 2016)

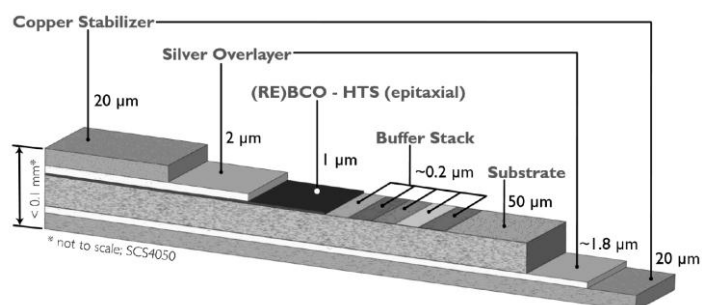


Fig. 2. The structure of second generation superconducting tape by SuperPower (SuperPower Inc., 2016)

Second generation superconducting tapes are usually made of YBCO material. It is a chemical compound comprising yttrium oxide, barium oxide and copper oxide. The general chemical formula of this material is $\text{YBa}_2\text{Cu}_3\text{O}_{6+x}$ ($0 < x < 1$). Figure 3 illustrates the single structure diagram of the superconducting powder.

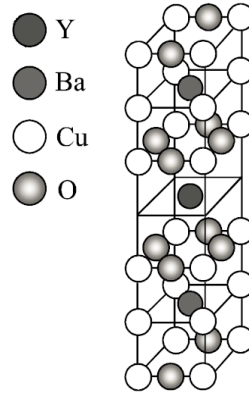


Fig. 3. Single structure diagram of superconducting powder $\text{YBa}_2\text{Cu}_3\text{O}_7$ (Parida, 2012)

3. NUMERICAL MODEL OF 2G YBCO SUPERCONDUCTING TAPE

3.1. Equivalent circuit of 2G YBCO superconducting tape

The modelling object is 2G YBCO superconducting tape. Figure 4 presents the equivalent circuit of the tape. Mathematical model of the superconducting tape consists of three non-linear and one linear resistor in parallel. These resistors include: Hastelloy, a silver layer, a copper layer and a superconducting layer (Czerwinski, Jaroszynski, Majka, Kozak, and Charnas, 2016; Jaroszynski & Janowski, 2014).

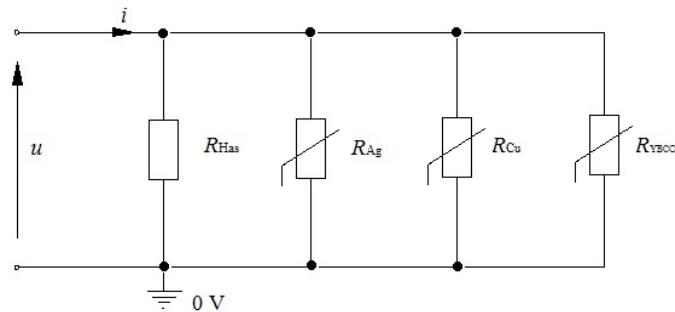


Fig. 4. Equivalent circuit of 2G YBCO superconducting tape

Equivalent diagram of the simulated circuit is shown in Figure 5. This circuit consists of the sinusoidal voltage source V_{\sin} , the internal resistance of the power source R_w and the temperature- and current-dependent resistance of the superconducting tape R_{HTS} .

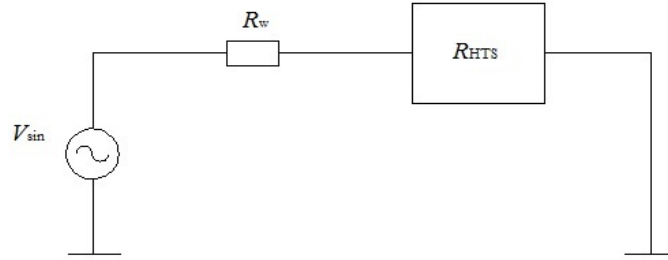


Fig. 5. Equivalent diagram of simulated circuit

3.2. Modelling tool

The model of 2G YBCO superconducting tape was created in the PSpice program. It is a well-known program for circuit design and simulation.

Orcad PSpice enables to:

- design schemes of the analysed circuit,
- choose types and values of elements,
- perform the simulation and display the results in a graphic form,
- use analogue behavioural modelling.

In comparison to circuit modelling finite element method (FEM) subdivides a large problem into smaller, simpler parts that are called finite elements. Due to the high geometric aspect-ratio of superconducting tape, this method leads to the much greater complexity of the calculations than circuit modelling in PSpice program. The second approach seems to be quite effective for the analysis of states when the transport current is higher than I_c (Czerwinski, Jaroszynski, Janowski, Majka, and Kozak, 2014; Janowski, Wojtasiewicz, and Jaroszynski, 2016; Jaroszynski et al., 2014).

PSpice program enables to examine the system for changes in such quantities as:

- voltage,
- current,
- power,
- temperature,
- additional parameters of the model.

3.3. Details of the simulation

The circuit model of 2G YBCO superconducting tape is designed in PSpice program. The model, presented in Figure 6, consists of a passive block PARAM containing the electrical, thermal and geometrical parameters of the tape, and active user blocks of the ABM (analogue behavioural modelling). Voltage blocks calculate the relative temperature (ABM1) in relation to the temperature of liquid nitrogen, the cooling (ABM2) and heating power (ABM3) of the superconducting tape, and the current block calculates the current of the tape (ABM4). For the purpose of current detection in the circuit a secondary DC source (Vpr) with zero voltage (EMF) was used. The model uses tables with the values of power density passed to the liquid nitrogen as the function of temperature (GeStCieLN) and two hierarchical blocks. The first hierarchical block represents thermal capacity (Cth), which is the sum of the thermal capacity of the layer of copper, silver, Hastelloy and the YBCO superconductor. The second hierarchical block calculates the resultant conductance of the tape (G). This block allows for a smooth transition of the YBCO superconductor layer into the resistive state in which the current is described by Rhyner's power law (1) (Czerwinski et al., 2016; Janowski et al., 2016; Jaroszynski et al., 2014).

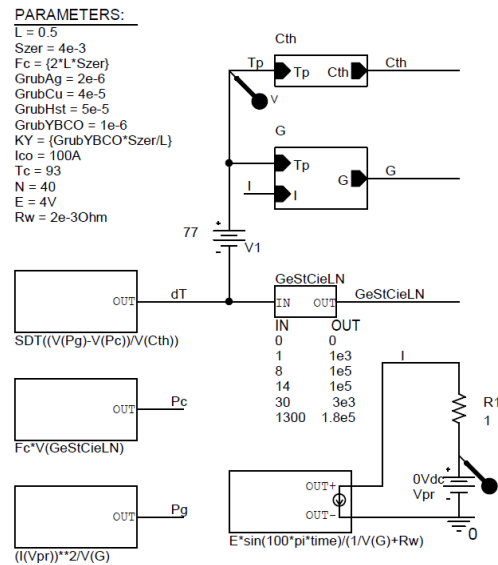


Fig. 6. Electrical circuit of 2G YBCO superconducting tape in PSpice

High temperature superconductors have a non-linear dependence of current density and electric field intensity. GYBCO block (Fig. 7) calculates resistance change (transition into the resistive state) of a superconducting layer in the second generation superconducting tape.

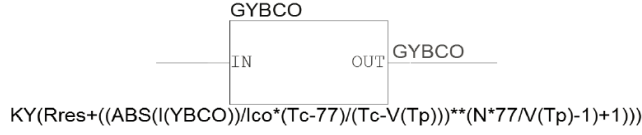


Fig. 7. ABM voltage block calculating the conductance of the YBCO superconducting layer

Exponential dependence (1) describes the relations between current density J and electric field intensity E

$$\frac{E}{E_c} = \left(\frac{J}{J_c(T)} \right)^{n(T)} \quad (1)$$

where: E – electric field intensity, V/m,
 E_c – critical electric field intensity for HTS, 10^{-4} V/m,
 J – current density, A/m²,
 J_c – critical current density, A/m²,
 n – exponent depending on the temperature.

The relation between electric field intensity and current density in power law depends on the actual temperature. The temperature affects the critical value of the current and the value of the exponent n . This exponent influences the steepness in rise of current-voltage characteristics and is defined for the purposes of the circuit modelling as:

$$n(T) = n_0 \frac{T_0}{T} \quad (2)$$

where: T_0 – reference temperature, K,
 T – temperature of tape, K,
 n_0 – exponent in T_0 temperature (for YBCO $n_0 = 15 \div 40$, $T_0 = 77$ K).

Assuming homogenous distribution of current density and electric field intensity, the equation (1) can be written as:

$$\frac{U}{U_c} = \left(\frac{I}{I_c(T)} \right)^{n_0 \frac{T_0}{T}} \quad (3)$$

where: U – voltage, V,
 U_c – critical voltage, V,
 I – current, A,
 I_c – critical current, A.

After multiplying components of the equation (3) the following dependence can be described as:

$$\frac{U}{I} = \frac{U_c}{I_c(T)} \left(\frac{I}{I_c(T)} \right)^{n_0 \frac{T_0}{T} - 1} \quad (4)$$

The dependence (4) can be presented in the form of resistance:

$$R_{YBCO} = \frac{U_c}{I_c(T)} \left(\frac{I}{I_c(T)} \right)^{n_0 \frac{T_0}{T} - 1} \quad (5)$$

where: R_{YBCO} – the resistance of YBCO layer, Ω .

Critical current $I_c(T)$ in the equation (5) can be illustrated by the linear relationship:

$$I_c(T) = I_{c0} \frac{T_c - T}{T_c - T_0} \quad (6)$$

where: T_c – critical temperature, K,

I_{c0} – critical current in T_0 temperature, A.

After substitution into the equation (5) the dependence (6) of critical current $I_c(T)$ the equation is:

$$R_{YBCO} = \frac{U_c}{I_c} \left(\frac{I}{I_{c0} \frac{T_c - T}{T_c - T_0}} \right)^{n_0 \frac{T_0}{T} - 1} \quad (7)$$

After including the critical electric field intensity, the equation is:

$$R_{YBCO} = \frac{E_c \cdot L}{I_c} \left(\frac{I}{I_{c0} \frac{T_c - T}{T_c - T_0}} \right)^{n_0 \frac{T_0}{T} - 1} \quad (8)$$

where: L – length of tape, m.

The conductance of the superconductor is the reciprocal of resistance:

$$G_{YBCO} = \frac{1}{R_{rez} + R_{YBCO}} \quad (9)$$

where: G_{YBCO} – the conductance of YBCO layer, S,

R_{rez} – residual resistance (a small value higher than zero needed to perform the convergent calculations, in this program equals $10^{-15} \Omega$).

3.4. Simulation results

The simulation takes into the account the following factors: the sinusoidal voltage source with the amplitude of 4 V, frequency 50 Hz and internal resistance $2 \cdot 10^{-3} \Omega$, the length of tape 0.5 m, the width of tape $4 \cdot 10^{-3}$ m, the thickness of a silver layer $2 \cdot 10^{-6}$ m, the thickness of a copper layer $4 \cdot 10^{-5}$ m, the thickness of Hastelloy $5 \cdot 10^{-5}$ m, the thickness of YBCO layer 10^{-6} m, the critical current of the tape $I_{C0} = 100$ A, the critical temperature of superconductor $T_C = 93$ K, the temperature of liquid nitrogen $T_0 = 77$ K, Rhyner's law exponent $n_0 = 40$.

3.4.1. Thermal capacity of 2G YBCO tape

The hierarchical block Cth (Fig. 8) enables to calculate the thermal capacity of 2G YBCO tape. This block comprises thermal capacity of a copper layer C_{thCu} , a silver layer C_{thAg} , Hastelloy C_{thHST} , YBCO superconductor C_{thYBCO} . The calculations are based on the dependence of the thermal capacity for individual layers of the tape as a function of temperature, as can be seen in Fig. 9, Fig. 10 and Fig. 11. This data allows to create tables with specific heats of copper layer C_{wCu} , silver layer C_{wAg} , Hastelloy C_{wHST} . The constant value of 185 J/(kg·K) is accepted as the specific heat for the superconducting layer C_{wHST} . The calculations also include the density γ of the individual layers in the superconducting tape, which are presented in Table 2.

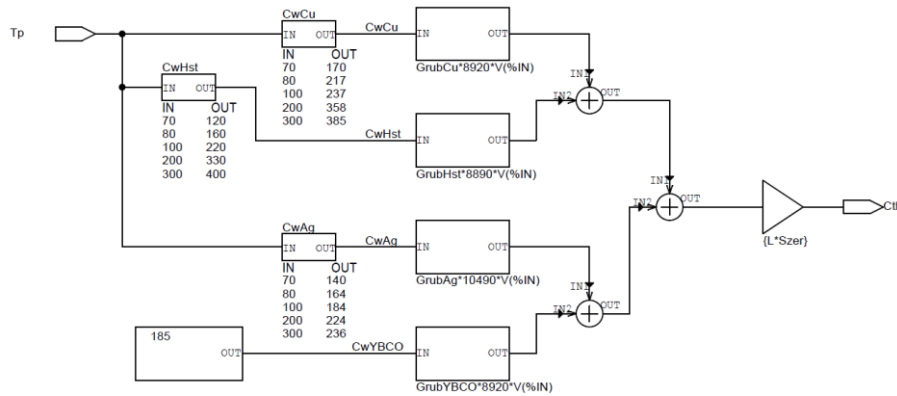


Fig. 8. Subcircuit calculating thermal capacity of 2G YBCO tape

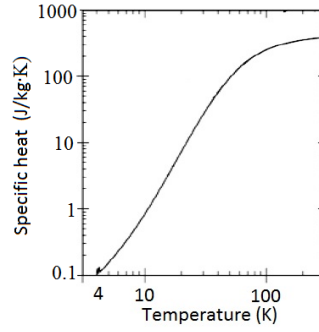


Fig. 9. Specific heat of copper vs. temperature (Matula, 1979)

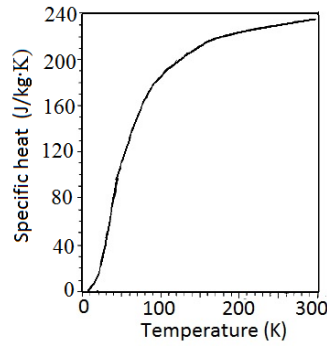


Fig. 10. Specific heat of silver vs. temperature (Smith & Fickett, 1995)

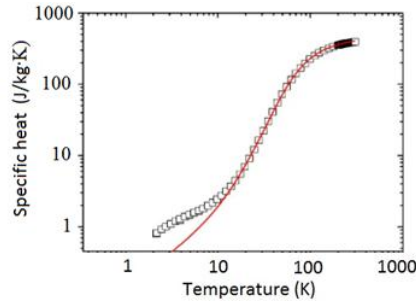


Fig. 11. Specific heat of Hastelloy vs. temperature (Lu, Choi, and Zhou, 2008)

Table 2. Material density of individual layers in the superconducting tape (Czerwinski et al., 2014)

γ_{Cu}	8920 kg/m ³
γ_{Ag}	10490 kg/m ³
γ_{YBCO}	6300 kg/m ³
γ_{HST}	8890 kg/m ³

3.4.2. The conductance of copper, silver, Hastelloy and YBCO layer

In this model the conductance of 2G YBCO tape is calculated using the hierarchical block G (Fig. 6). The calculations are based on the dependence in the resistivity ρ of copper and silver layers as a function of temperature, which are presented in Fig. 12 and Fig. 13. The resistivity for Hastelloy is of constant value and equals $1.24 \cdot 10^{-6} \Omega\text{m}$. The calculations also include the thickness of individual layers, as well as the length and the width of the superconducting tape. The developed conductance model of 2G YBCO tape was used for generating conductance waveforms of copper layer G_{Cu} , silver layer G_{Ag} , Hastelloy G_{HST} (Fig. 14).

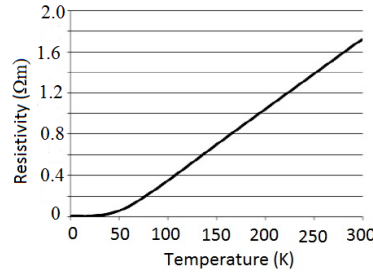


Fig. 12. Change of copper resistivity vs. temperature (Matula, 1979)

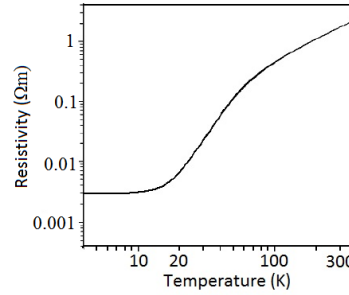


Fig. 13. Change of silver resistivity vs. temperature (Smith et al., 1995)

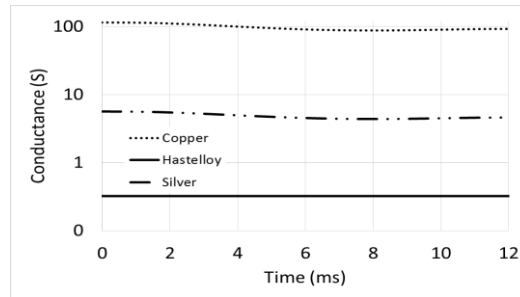


Fig. 14. Conductance waveforms of copper layer G_{Cu} , silver G_{Ag} , Hastelloy G_{HST} vs. time

Due to the large differences in conductance of individual layers in the superconducting tape, waveforms have been developed on a logarithmic scale. The values of conductance for copper layer G_{Cu} , silver layer G_{Ag} and Hastelloy G_{HST} are constant in the analysed time and have values respectively of 100 S, 8 S, 0.5 S.

Figure 15 presents the conductance waveforms of YBCO superconducting layer vs. time.

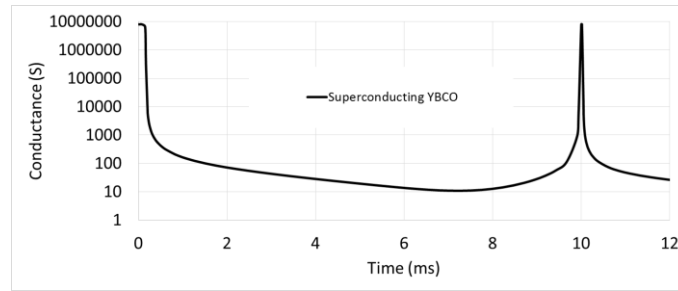


Fig. 15. Conductance waveforms of superconducting layer G_{YBCO}

The conductance of the superconducting layer G_{YBCO} reaches the maximum about 8 MS when the current in the circuit tends to zero.

3.4.3. The current of copper, silver, Hastelloy and YBCO layer

The controlled current source was used for each layer of the superconducting tape, which allowed to calculate the instantaneous current of individual layer. Figure 16 illustrates the initial current waveforms in the copper layer I_{Cu} , silver layer I_{Ag} , Hastelloy I_{HST} , YBCO I_{YBCO} and total current of superconducting tape I_{HTS} . Tape current I_{HTS} in a longer span is also depicted in Figure 17.

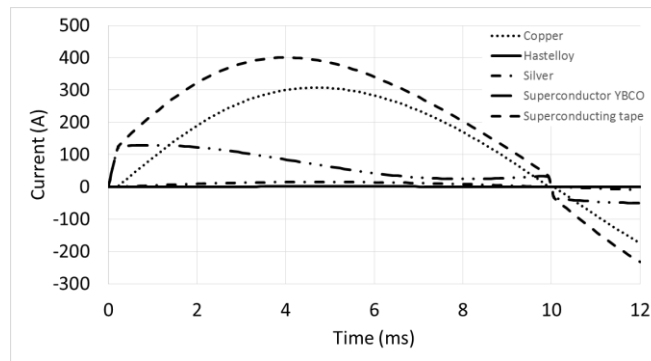


Fig. 16. Current waveforms in copper layer I_{Cu} , silver I_{Ag} , Hastelloy I_{HST} , superconductor I_{YBCO} and the total current of superconducting tape I_{HTS} vs. time

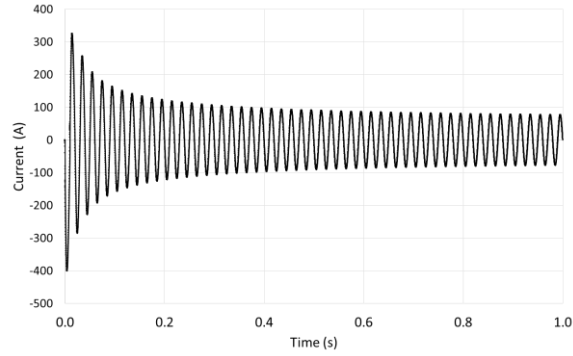


Fig. 17. Waveform of the total current of superconducting tape I_{HTS}

After setting the supply voltage in a period of time (0 – 0.2 ms) the current flows only through YBCO layer. The maximum of current I_{YBCO} is about 120 A and then, starts to decrease due to the fast heating of the tape. The copper layer allows for the flow of current I_{Cu} at the maximum 300 A. The peak current of superconducting tape I_{HTS} is 405 A. This value is reached in 4 ms. After 300 ms current I_{HTS} proceeds to the quasi-steady state, the amplitude is less than 100 A. The silver and Hastelloy layers conduct relatively small currents of about a few amperes.

3.4.4. Temperature, heating and cooling power of superconducting tape

Figure 18 presents a six-element table GeStCieLN with the values of heat flux density (W/m^2) passed to the liquid nitrogen vs. temperature difference ΔT . The table was based on the dependence of the heat flux density passing through the metal surface and the liquid nitrogen vs. temperature difference ΔT (Fig. 19).

GeStCieLN		GeStCieLN	
IN	OUT	IN	OUT
0	0	0	0
1	1e3	1	1e3
8	1e5	8	1e5
14	1e5	14	1e5
30	3e3	30	3e3
1300	1.8e5	1300	1.8e5

Fig. 18. Six-element table with heat flux density passed to the liquid nitrogen vs. temperature difference ΔT

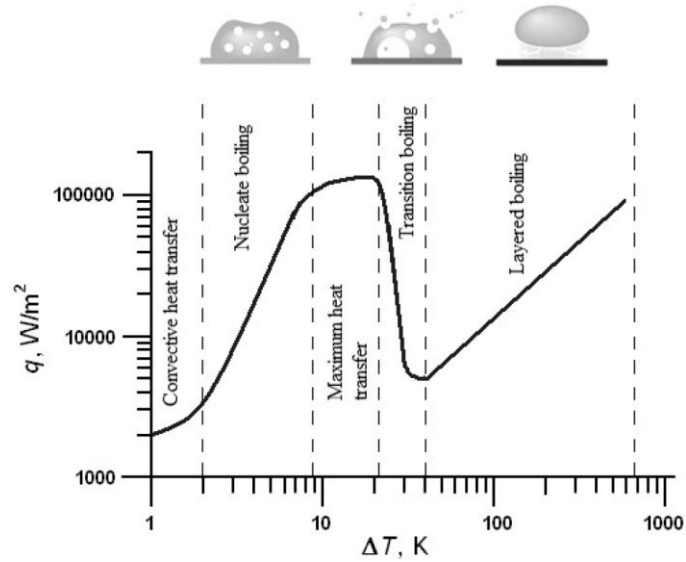


Fig. 19. Heat flux density passing between the metal surface and liquid nitrogen bath vs. temperature difference ΔT (Lu J. et al., 2008)

Figure 6 shows voltage blocks calculating change of temperature (ABM1) in relation to the temperature of liquid nitrogen, the cooling power (ABM2) and the heating power of superconducting tape (ABM3).

The change in temperature, cooling and heating power of superconducting tape vs. time are presented respectively in Fig. 20 and Fig. 21.

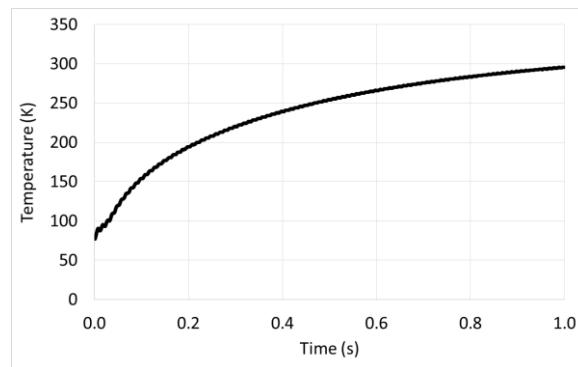


Fig. 20. Temperature of superconducting tape as a function of time

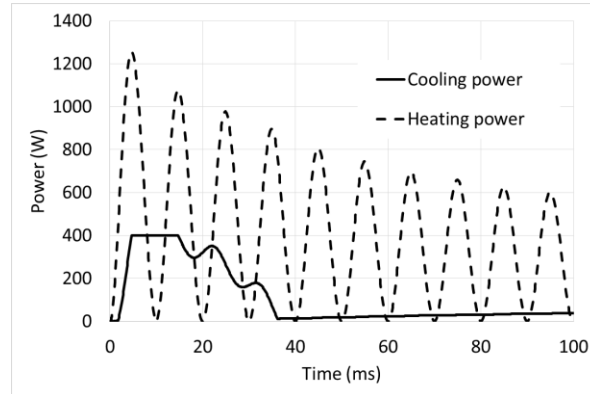


Fig. 21. Heating power and cooling power of the superconducting tape in a function of time

The temperature of superconducting tape increases and after 1 s it reaches the highest value $T = 293$ K. The maximum cooling power of the superconducting tape equals 400 W. The peak heating power of the tape is 1.45 kW, and during the experiment decreases to about 0.57 kW.

4. CONCLUSIONS

The rapid growth in information technology, the development of software and the computer calculations make the computer simulations one of The basic tools to examine and analyse the physical devices and phenonema.

PSpice program allows to design computer models of superconducting elements.

Blocks of the ABM (analogue behavioural modelling) in electronic circuit simulation enable to analyse the transients of the superconducting tape which is used in the windings of superconducting transformers.

Thanks to PSpice program and active user blocks of behavioural modelling, the electrical circuit simulation seems to be a reliable tool for the analysis of superconducting materials in transitional conditions.

REFERENCES

- American Superconductor*. (n.d). Retrieved December 2, 2016, from AMSC website, http://www.amsc.com/solutions-products/YBCO_wire.html
- Czerwinski, D., Jaroszynski, L., Janowski, T., Majka, M., &Kozak, J. (2014). Analysis of Alternating Overcurrent Response of 2G HTS Tape for SFCL. *IEEE Transactions on Applied Superconductivity*, 24(3), 5600104. doi:10.1109/TASC.2013.2281494

- Czerwinski, D., Jaroszynski, L., Majka, M., Kozak, J., & Charnas, B. (2016). Comparison of Over-current Responses of 2G HTS Tapes. *IEEE Transactions on Applied Superconductivity*, 26(3), 5602904. doi:10.1109/TASC.2016.2520080
- Janowski, T., Wojtasiewicz, G., & Jaroszynski, L. (2016). Short-circuit current limitation by superconducting transformer. *13th Selected Issues of Electrical Engineering and Electronics (WZEE)*. doi:10.1109/WZEE.2016.7800231
- Jaroszynski, L., & Janowski, T. (2014). YBCO coated conductors for superconducting transformer windings. *Przegląd Elektrotechniczny*, 90(1), 164–166. doi:10.12915/pe.2014.01.39
- Lu, J., Choi, E. S., & Zhou, H. D. (2008). Physical properties of Hastelloy C-276TM at cryogenic temperatures. *Journal of Applied Physics*, 103, 064908. doi:10.1063/1.2899058
- Majka, M., & Kozak, S. (2009). Zastosowanie taśm I i II generacji do budowy nadprzewodnikowych ograniczników prądu. *Przegląd Elektrotechniczny*, 87(5), 183–185.
- Matula, R. A. (1979). Electrical resistivity of copper, gold, palladium and silver. *Journal of Physical and Chemical Reference Data*, 8(4), 1147-1298. doi:10.1063/1.555614
- Parida, B. (2012). DC electrical resistivity studies in bulk YBCO/Ag composites. *A report submitted to Department of Physics National Institute of Technology, Rourkela*.
- Smith, D. R., & Fickett, F. R. (1995). Low-Temperature Properties of Silver. *Journal of Research of the National Institute of Standards and Technology*, 100(2), 119–171.
- SuperPower Inc. (n.d.). Retrieved December 2, 2016, from SuperPower Inc. website, <http://www.superpower-inc.com/content/2g-hts-wire>
- Tinkham, M. (2004). *Introduction to Superconductivity (2nd ed.)*. Dover Books on Physics.

kinematic analysis, nonuniformity, piston motion, radial engine

Konrad PIETRYKOWSKI, Tytus TULWIN**

THE NONUNIFORMITY OF THE PISTON MOTION OF THE RADIAL ENGINE

Abstract

The results of kinematic analysis of the ASz-62IR radial engine crankshaft was presented. In addition, the one-dimensional model of the working cycle of the engine was created in AVL BOOST system. Differences in the waveforms for each pistons causes the differences in the filling process what reflects in the mass of the load supplied to cylinders. Additionally, due to one dimensional model computation. The results show differences in the value of maximum pressure. This causes differences in mean effective pressure of up to 4% and which also affects the vibrations of the whole engine.

1. INTRODUCTION

The radial engines are used in aviation for a long time, mainly due to the simple design, high reliability and low purchase and operation costs. There used to be a source of power system in most aircrafts. Gradually, they has been replaced by gas turbine engines, however, they are still used in certain groups of aircraft, including airplanes used in agriculture and by firefighters and they are still produced. This is mainly due to the relatively low costs of production, operation, reliability and simple surveys of those radial engines. They are still ongoing works to improve their performance. An example is ASz-62IR engine (Fig. 1) produced by the Polish Aviation Company PZL Kalisz and mounted in the M-18 Dromader and An-2 aircrafts, in which the carburetor has been replaced by fuel injection system into inlet pipes. This allows to fuel consumption reduction. The system also enables to supply the engine with an automobile petrol. Comparison of the performance of an engine running on different fuels is presented by Czarnigowski, Jakliński, and Wendeker (2010).

* Department of Thermodynamics, Fluid Mechanics and Aviation Propulsion Systems, Faculty of Mechanical Engineering, Lublin University of Technology, Nadbystrzycka Street 36, 20-618 Lublin, Poland, +48 815384764, k.pietrykowski@pollub.pl, t.tulwin@pollub.pl

One of the major disadvantages of radial engines are high value of vibrations. They cause rapid wear of engine parts and load to aircraft design. One of the vibration causes is nonuniformity of individual cylinders of the radial engine, which is due to its specific structure. Works on the diagnostic method of this phenomenon, based on statistical nonlinear analysis of time series in radial engine were conducted by Gęca, Litak, Wendeker, Jakliński, Czarnigowski, and Pietrykowski (2009). This phenomenon, combined with the specific construction of the engine, results in an uneven heat load in the cylinders (Tulwin, 2016), and (Pietrykowski & Tulwin, 2015). However, the literature does not explain the impact of this phenomenon on the engine work process. This was the motivation to explain this phenomenon.

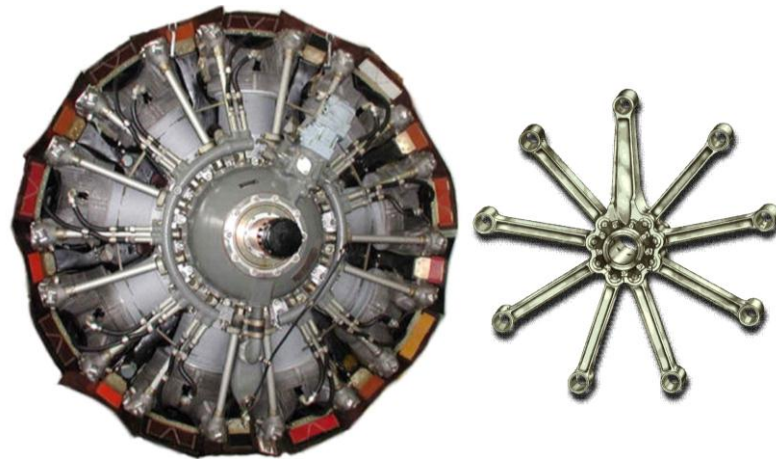


Fig. 1. AS-62IR engine and assembly of connection rods

The object of the research is a 9-cylinder aircraft radial engine named ASz-62IR. The engine is air-cooled and supercharged by radial compressor. Engine performance data are shown in Table 1.

Tab. 1. ASz-62IR engine performance

Power	746 kW (1000 HP) 2200 RPM
Compression ratio	6.4:1
Fuel consumption	about 200 l/h
Specific Fuel Consumption	469 g/(kWh)
Power/Mass	1.3 kW/kg

2. PISTON MOTION MODELL

2.1. Piston motion equation

In radial engine, determination of the piston position is easy for the first piston, since the main connecting rod (master rod) is connected directly to the crankshaft, as in most piston engines. The situation becomes more complicated, when we consider the motion of the other pistons of a radial engine, whose connecting rods (articulated rods) are connected to the master rod.

To mapping of the motion course of the individual pistons with the specific characteristics of the radial engine crank-piston system uses the equation (1) developed by Sibert (1940). It should be noted that the formula provides for simplification of the angle $\alpha = \beta$, and relationship $l + r = L$ does not have to be fulfilled. These assumptions are correct for the ASz-62IR engine.

Figure 2 shows a kinematic diagram of the master rod and one of the articulated rod. Point O is the center of the crankshaft, P and P' are the pivot points of connecting rod little end, C and C' are the pivot points of connecting rod big end. Line OP' = S', is the search position of piston pin of any of the pistons. Then, as shown in Figure 2:

$$S' = R \cos (\theta - \beta) + r \cos \varphi + l \cos \varphi' \quad (1)$$

Equation (1) was used to calculate S' as φ and φ' can be determined from the relationship:

$$L \sin \varphi = R \sin \theta \quad (2)$$

$$l \sin \varphi' = R \sin (\theta - \beta) + r \sin \varphi \quad (3)$$

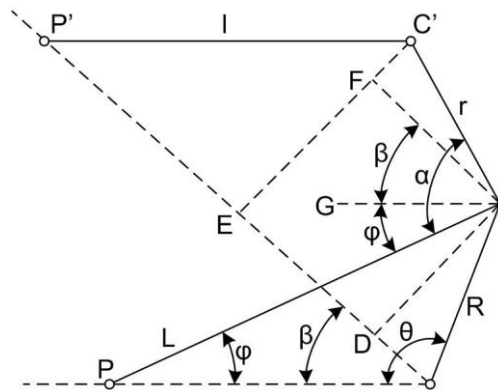


Fig. 2. Scheme of crank-piston system (Sibert, 1940)

In order to perform the calculations, it was necessary to add parameters of the model. They result from the dimensions of the crank-piston system of ASz- 62IR engine. They were obtained from the technical drawings of elements of the crank-piston system and shown in Table 2.

Tab. 2. The dimensions of the ASz-62IR engine crank-piston system

Cylinder no	1	2	3	4	5	6	7	8	9
R [mm]	87.25	87.25	87.25	87.25	87.25	87.25	87.25	87.25	87.25
l	349.25	274.62	274.62	274.62	274.62	274.62	274.62	274.62	274.62
r [mm]	0	76.098	77.792	76.961	75.002	75.002	76.961	77.792	76.098
β [mm]	0	40	80	120	160	200	240	280	320

2.2. Verification of the model of the piston motion

In order to validate the analytical model of the pistons motion model, a kinematic model in CATIA v5 was built (Fig. 3). CATIA v5 is a program from a group of CAD (Computer Aided Design) software for creating 2D and 3D geometry models. Sketcher module allows to quickly explore dependences of the geometry in complex physical model. It does not allow to find solutions in the form of analytical equations, but allows to verify them in the selected points. The dimensions of the elements in Figure 3 were taken from Table 2.

The results of calculations for different angles for all the cylinders were compared with the values read from the piston positions of the kinematic model, what showed full compliance of both models. The model can be used to calculate the course of motion of the pistons.

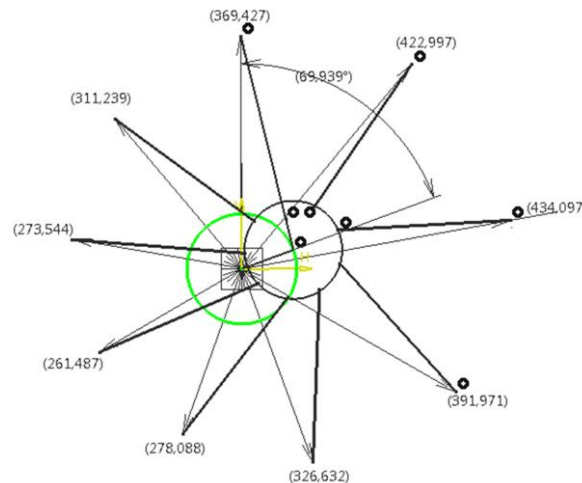


Fig. 3. The kinematic model of the crank-piston system of ASz-62IR engine

3. 1D ENGINE WORKING CYCLE MODEL

To examine the effect of the crank-piston system geometry on work of radial engine, a 1-dimensional model of the ASz-62IR engine was built in AVL BOOST system. This software is a tool dedicated for 1-dimensional modeling of internal combustion engines. This program uses a zero-dimensional physical modeling, based on the principle of laws of conservation of mass and energy. This approach allows for mapping of the processes in the internal combustion engine and the parameters of the working medium in the cylinder, for the defined conditions, while speeding up the calculations as compared to three-dimensional models. AVL BOOST allows to analyze the impact of design configuration for engine performance (power, torque, fuel consumption, etc.).

AVL Workspace Graphical User Interface is a tool for pre-processing, that includes a model editor and a system for import external data, necessary to simulate and compare results. Model creation is based on choosing the block elements, forming the structure of the engine and connecting them by segments, serving as conductors of circular cross-section. With this approach it is possible to create and modify even the most complex models, consisting of many components.

Engine model (Fig. 4) consists of an intake system, including the compressor, the cylinders and the exhaust gas system. Compressor model includes a map that takes into account the dependence of pressure ratio and efficiency from the mass flow and rotational speed. The dimensions of the flow elements were obtained from the construction drawings of the engine. In order to obtain correct model, the characteristics of valves lift were introduced into the cylinder.

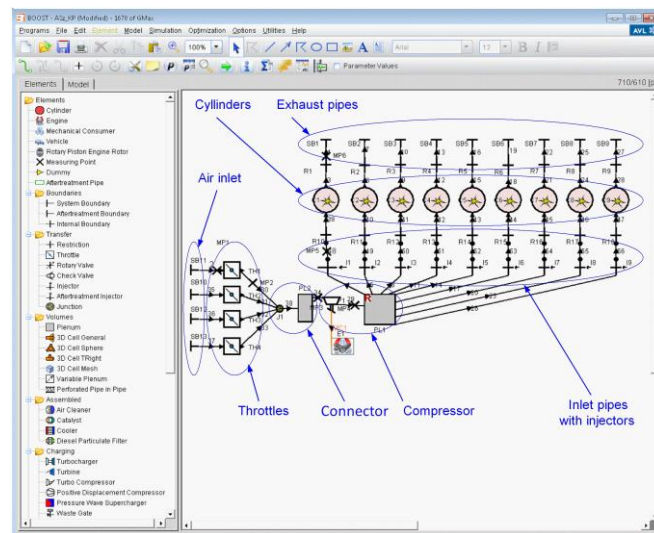


Fig. 4. 1D model of ASz-62IR engine (Pietrykowski & Gęca, 2014)

Combustion model was defined using Vibe function (Fig. 5). Model parameters are the same for all cylinders. Detailed description of the engine model is presented in paper of Pietrykowski, and Gęca (2014).

An important function of the AVL BOOST system is the ability to independently define any course of motion of any piston. The motion of the piston of the first cylinder is determined by the software based on the dimensions of the crank-piston system. The other characteristics of cylinders were made using text files containing waveforms calculated by the analytical model.

4. RESULTS

4.1. Pistons positions

Based on the equations of the piston motion and the dimensions of the ASz-62IR engine crank-piston system (Table 1 and 2), the calculations of ASz-62IR engine pistons motion was made. Figure 5 shows the calculated characteristics of position of the pistons.

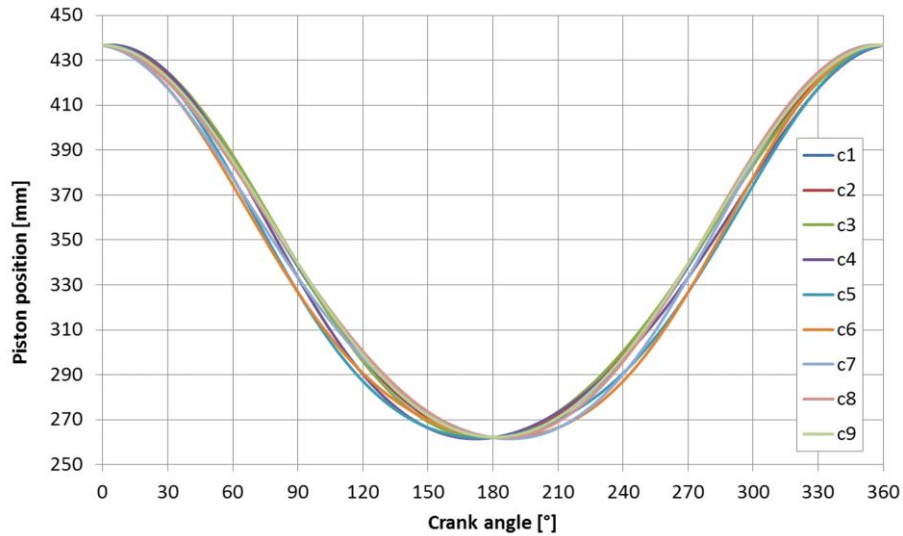


Fig. 5. Characteristics of position of the piston

In the drawings 6 and 7 the characteristics of position of the pistons are also shown, however, the scale is adjusted in this way to show the differences in the angles of incidence of the upper and bottom dead center of the piston. The maximum difference between the bottom dead center positions of the pistons is 0.72 mm and between top dead center positions is 0.3 mm. These differences

are not large enough to significantly affect the degree of compression or pistons stroke and cause variation of the combustion process in each cylinder. The other situation occurs in the angle value of the top dead center position of the pistons. The maximum difference occurs between the cylinders 4 and 7, and is 7.6 CAD causing a significant shift in ignition timing in most cylinders according to TDC. Moreover, different velocities of the pistons during the filling process can result in different mixture mass provided to the individual cylinders.

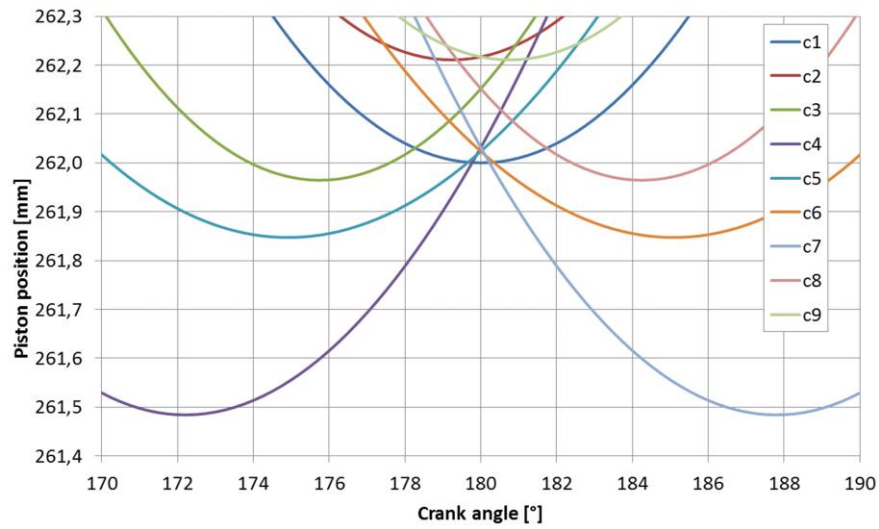


Fig. 6. Characteristics of position of the pistons (near BDC)

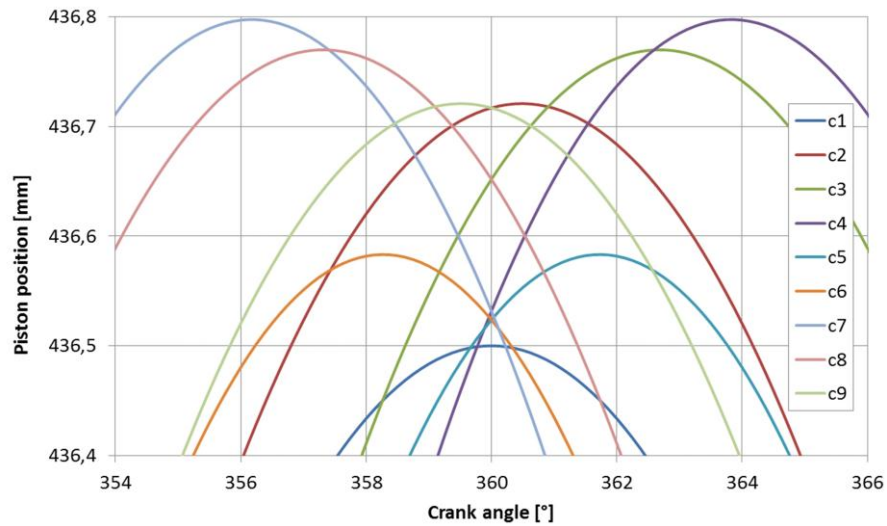


Fig. 7. Characteristics of position of the pistons (near TDC)

4.2. Engine work process

Figure 8 shows the calculated characteristics of pressure in the cylinders of the radial engine. There were no significant differences in compression pressure, but there are differences in the maximum pressure values. This is a result of different combustion process in each cylinder. This phenomenon can be observe in the radar scheme (Fig. 9) showing the percentage deviation from mean indicated pressure in comparison to the first cylinder. The maximum difference is 4% and occurs between the cylinders 5 and 7.

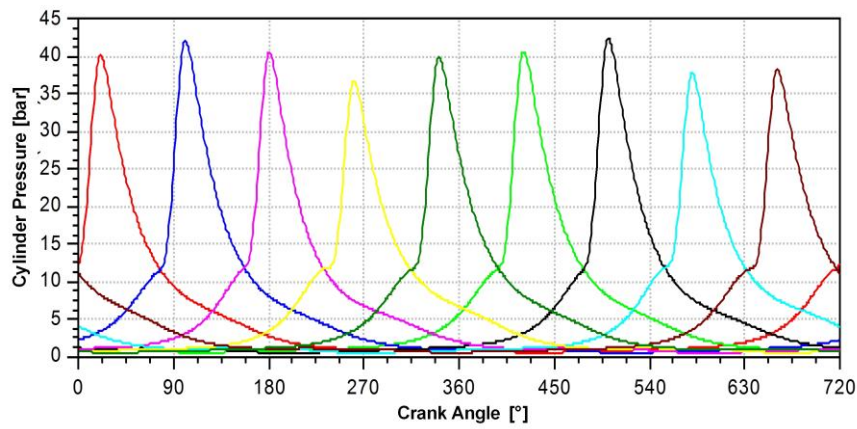


Fig. 8. Characteristics of pressure in the cylinders

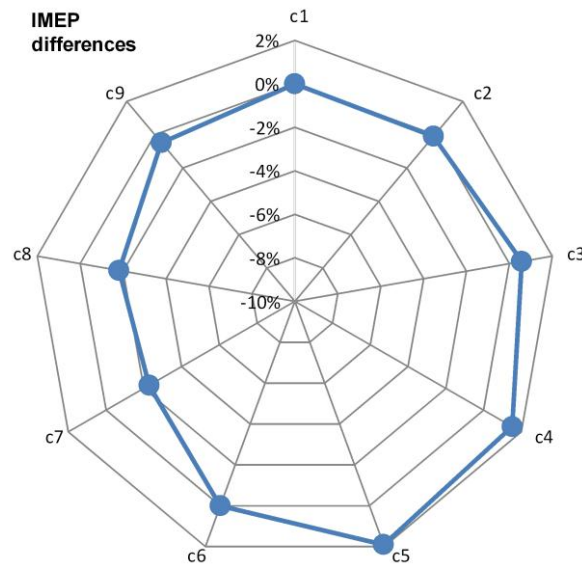


Fig. 9. Distribution of IMEP for each cylinder

5. CONCLUSIONS

Cylinder-to-cylinder variation in radial engines and resulting vibrations have been known for a long time. Now, advanced software enables us to perform a qualitative evaluation of the impact of rod-crank system's kinematics on engine performance.

The 1D model, built in the AVL BOOST software, allows to quickly perform calculations and prediction of radial engine performance. Software enables to check the influence of the specific crank-piston system on the cylinders pressure. The difference in IMEP are 4%, resulting in variation of power generated by the individual cylinders and contributes to engine vibrations.

This phenomenon can be overcome by individual ignition control in every cylinder. However, this requires a replacement of the ignition system for electronically controlled. Radial engines are fitted with a magneto ignition system which is a simple and reliable solution. Today's electronic solutions also enable the required reliability and regulation of ignition timing for each cylinder and operating conditions to improve engine performance and increase the TBO.

Our further 1D-model research will be for varied ignition timing. There will be also a test bench at a dynamometer.

This work has been financed by the Polish National Centre for Research and Development, under Grant Agreement No. EPOCA INNOLOT/I/NCBIR/2013.

REFERENCES

- Czarnigowski, J., Jakliński, P., & Wendeker, M. (2010). Fuelling of aircraft radial piston engines by ES95 and 100LL gasoline. *Fuel*, 89(11), 3568–3578. doi:10.1016/j.fuel.2010.06.032
- Gęca, M., Litak, G., Wendeker, M., Jakliński, P., Czarnigowski, J., & Pietrykowski, K. (2009). Diagnostics of a combustion process in the aircraft radial engine. *PAMM Proceedings in Applied Mathematics and Mechanics*, 9, 677–678. doi:10.1002/pamm.200910308
- Pietrykowski, K., & Gęca M. (2014). Simulation studies of the aircraft radial engine. *Logistyka*, 6, 8645–8653.
- Pietrykowski, K. & Tulwin, T. (2015). Aircraft Radial Engine CFD Cooling Model. *SAE Int. J. Engines*, 8(1), 82–88. doi:10.4271/2014-01-2884
- Siebert, H. W. (1940). Approximate Formulas for Piston Travel in Radial Engines. *Journal of the Aeronautical Sciences*, 7(10), 434–437. doi:10.2514/8.1194
- Tulwin, T. (2016). A coupled numerical heat transfer in the transient multicycle CFD aircraft engine model. *Procedia Engineering*, 157, 255–263. doi:10.1016/j.proeng.2016.08.364

*data envelopment analysis, non-parametric optimization,
dynamic problems, window analysis*

Svetlana RATNER^{}, Pavel RATNER^{**}*

DEA-BASED DYNAMIC ASSESSMENT OF REGIONAL ENVIRONMENTAL EFFICIENCY

Abstract

We apply window Data Envelopment Analysis (DEA) to the solution of the problem of assessment of the efficiency of regional production systems in Southern Russia. The proposed method allows to monitor the changes in efficiency of regional economic systems throughout time and has a high discrimination power. The simplicity of the technical implementation of the proposed method and the availability of the necessary software for its use allow one to hope for its wide implementation in the modern practice of regional environmental management.

1. INTRODUCTION

Data Envelopment Analysis (DEA) currently represents a developed methodology for comparative evaluation of efficiency of different production facilities using a wide range of input and output parameters. Efficiency, in the context of DEA, is the ratio of the weighted sum of production outputs (that is to say, production results such as volumes of produced goods) to a weighted sum of inputs (resources consumed), which allows to classify decision making units (DMUs) as effective only if they produce the maximal possible outputs with the minimal possible inputs (Charnes, Clarke, Cooper & Golany, 1984). Basic and modified data envelopment analysis models have been successfully employed to solve a wide variety of practical management tasks,

^{*} Institute of Control Science, Russian Academy of Science, 65 Profsoyuznaya st., Moscow 117997, Russia, +74953348910, lanarat@ipu.ru

^{**} Institute of Control Science, Russian Academy of Science, 65 Profsoyuznaya st., Moscow 117997, Russia, +74953348910, ratner.p.d.@gmail.com

from forming company or regional ratings, as well as ratings for innovative scientific programs to choosing optimal ways to increase the efficiency of DMUs which are currently ineffective (Khrustalev & Ratner, 2015a,b; Melnikov, 2016; Carrillo & Jorge, 2016). DMUs can represent both individual agents and some kinds of integrated formations such as corporations, clusters or regional economic systems, as long as their activities can be represented with the same sets of inputs and outputs.

One of the main factors that led to DEA becoming popular as a research method is availability of various software that allows to decrease the complexity of solving real-world problems to a minimum. Some freely available packages include DEA Frontier, MaxDEA, Open Source DEA, et al. They allow to use input- and output-oriented radial models with constant and variable return-to-scale. However, some more complex DEA options, such as those that allow to research efficiency of DMUs dynamically, are implemented as paid options in the aforementioned packages.

The most commonly used method involves calculating the Malmquist index (Malmquist, 1953; Fare et al., 1994). In contrast to a simple comparison of efficiency coefficients for each DMU during the times t and $t+1$ (which are calculated by solving two separate DEA problems), using the Malmquist index allows to also consider the change in the efficiency frontier itself, which can happen sometime during the period between t and $t+1$. In this case, the complexity of the problem and the volume of necessary calculations greatly increase.

To overcome these difficulties and to reduce the problem of monitoring the efficiency of objects dynamically down to solving two or more basic DEA models, one can use an approach known as "window analysis" (Charnes et al., 1985), which is similar to the moving average method. The idea of this method is to select a "window" for each DMU of width w , for example, $w=4$ for quarterly production data. Then each set of input and output data between 1 and w represents a single DMU, that is to say, the problem of evaluation efficiency is solved for $w \times n$ "DMUs", and for each real DMU w efficiency coefficients are calculated. The window is then moved by one observation to the right and w efficiency coefficients are re-calculated again for each DMU. In the end, one can use a simple arithmetic mean of the efficiency coefficients calculated for the specific time with different windows as the dynamic measure of efficiency. This approach allows for robust efficiency measurement and finding trends in DMU efficiency changes while remaining within the framework of basic DEA models that are freely available.

We test window analysis method while solving a problem of comparative ecologic&economic efficiency evaluation for regional economic system (RES). A static case was considered in (Ratner, 2016), where efficient regions are those that produce the most useful economic and social effects (interpreted as GRP and population) with minimal negative environmental impact (air, water and soil pollution). This paper presents a dynamic case of the same problem.

We solve the problem of monitoring efficiency of RES dynamically by calculating efficiency coefficients for each RES using window analysis with varying window widths. Comparing these results allows to conclude that using the maximal window width for window analysis is preferable both from the computing and content points of view.

2. METHODOLOGY

2.1. Basic environmental DEA model for assessment regional ecology management system's efficiency

Let's consider the task of evaluating ecologic and economic efficiency of regional economic systems (RES) using a set of indicators for the time period T . To do so, we need to use a basic input-oriented ecologic DEA (EDEA) model (Fare & Grosskopf, 2004) for each moment t in T . The difference between EDEA and traditional DEA lies in the presence of unwanted outputs. For each $t \in (1, \dots, T)$ we'll represent each RES as a DMU that uses various resources (energy, raw materials, labor, capital, etc.) as inputs and an economic result as an output. This can be measured with a variety of widely-used indicators, such as the GRP, gross value added, population's levels of income, etc. Furthermore, each DMU also outputs negative ecologic effects as an unavoidable result of economic activity: atmosphere pollution, solid waste, waste water, etc. For each RES _{t} , we look for a way to reduce the inputs (use of resources) and unwanted outputs (negative ecologic effects) without reducing desirable outputs (economic results). DMUs that produce maximal results with minimal negative ecologic effects and resource consumption during the moment t are considered effective.

This problem can be formalized thusly. Let there be K homogenous DMUs, each of which is defined with N inputs and M outputs. Outputs 1, 2, ... p are desirable (useful results) and outputs $p+1, p+2, \dots, M$ are undesirable (negative effects).

In the coefficient form, the problem of evaluating the efficiency of the 0-th DMU in moment t can be written down as:

$$\max_{u,v} \sum_{m=1}^M u_m y_{m0}^t \quad (1)$$

s.t.

$$\begin{aligned}
\sum_{m=1}^M u_m y_{mk}^t - \sum_{n=1}^N v_n x_{nk}^t &\leq 0 \quad k = 1, 2, \dots, K, \\
\sum_{n=1}^N v_n x_{no}^t &= 1, \\
u_m, v_n &\geq 0 \quad m = 1, 2, \dots, M \quad n = 1, 2, \dots, N;
\end{aligned}$$

where: $X^t = (x_{10}^t, \dots, x_{No}^t) \geq 0$ is a vector of inputs for the moment t of size N ,
 $Y^t = (y_{1o}^t, \dots, y_{Mo}^t) \geq 0$ is a vector of outputs for the moment t of size M ,
 K is the number of DMUs,
 u_m, v_n are unknown non-negative weights that need to be determined.

For each DMU, we solve a rational linear programming task to maximize the following:

$$h = \frac{\sum_{r=1}^p \mu_r y_{ro}^t - \sum_{s=p+1}^N \mu_s y_{so}^t}{\sum_{i=1}^M v_i x_{io}^t}, \quad (2)$$

s.t.

$$\frac{\sum_{r=1}^p \mu_r y_{rj}^t - \sum_{s=p+1}^N \mu_s y_{sj}^t}{\sum_{i=1}^M v_i x_{ij}^t} \leq 1$$

The ratio (2) is called the momentary efficiency measure for ecologic and economic efficiency of a DMU. DMUs that have this coefficient equal to 1 in moment t are effective, and the others are not. After calculating efficiency coefficients for every RES for each $t \in (t_1, \dots, T)$, we can examine the trends of the resulting dynamic series.

Undesirable outputs can simply be viewed as inputs; thus the momentary efficiency measure becomes:

$$h^* = \frac{\sum_{r=1}^k \mu_r y_{ro}^t}{\sum_{i=1}^M v_i x_{io}^t + \sum_{s=k+1}^p \mu_s y_{so}^t}, \quad (3)$$

Well known study of Korhonen and Luptacik (2004) proves that the ecologic and economic efficiency h и h^* are equivalent and can both be used to solve basic CCR models, while other authors (Ratner, 2016; Khrustalev and Ratner, 2015a,b; Fare & Grosskopf, 2004) show that in a simple case, undesirable outputs can be used as the only inputs for a model.

This interpretation of undesirable outputs is quite justified when solving a problem that doesn't require tracking the efficiency of each type of resource used by the RES (Ratner, 2016; Khrustalev & Ratner, 2015b). This simplified version of the problem marks the DMUs that produce the maximal social and economic results with the minimal negative ecological effects as efficient. The set of these DMUs defines a hyperplane of a convex multifaceted cone. DMUs that have efficiency coefficients below one can have their inputs proportionally reduced to move closer to the efficiency barrier: $(X_0^t, Y_0^t) \Rightarrow (hX_0^t, Y_0^t)$ (Cook & Seiford, 2009).

One can obtain an efficient point from the original one using the slack variables $S^+(s_1^+, \dots, s_N^+)$ and $S^-(s_1^-, \dots, s_M^-)$ by performing a shift $(hX_0^t - S^-, Y_0^t + S^+)$. These slack variables are determined during the second stage of solving the optimization problem and are interpreted as the potential decrease for negative ecologic effects. Some sources call this step of calculating the additional variables a "goal-setting method" (Bian et al., 2013), since the calculated potentials are the goals for each DMU's efficiency. Using dynamic series for each of the target parameters also gives a lot of additional information for DMUs in ecologic management and economic systems.

2.2. Dynamic environmental DEA model for assessment regional ecology management system's efficiency

Window analysis is a widely-used method for evaluating changes in DMU efficiency throughout time. This method allows to compare the DMU being examined not only with other DMUs but also with itself in other time periods. To do so, each of the K DMUs is represented as a set of T homogenous DMUs $DMU_i^{t_1}, DMU_i^{t_2} \dots DMU_i^{t_T}$, defined by inputs $X_i^{t_1}, X_i^{t_2}, \dots, X_i^{t_T}$ and outputs $Y_i^{t_1}, Y_i^{t_2}, \dots, Y_i^{t_T}$. The DEA problem (1) is then solved $T-w+1$ times for $K \times w$ ($w \leq T$) DMUs (or, in the context of these research, regions) $DMU_1^{t_j}, DMU_1^{t_j+1}, \dots, DMU_1^{t_j+w}, \dots, DMU_K^{t_j}, DMU_K^{t_j+1}, \dots, DMU_K^{t_j+w}$.

The first time, problem (1) is solved for the time interval of $t_1, \dots, t_1 + w$. Let us define this interval as w_1 . Solving this problem $\forall DMU_i$ we calculate w coefficients of momentary efficiency $h^{t_1}(X_i^{t_1}, Y_i^{t_1}), h^{t_1+1}(X_i^{t_1+1}, Y_i^{t_1+1}), \dots, h^{t_1+w}(X_i^{t_1+w}, Y_i^{t_1+w})$, that correspond to $DMU_i^{t_1}, DMU_i^{t_2} \dots DMU_i^{t_1+w}$.

The window is then moved by one interval to the right. The second time we solve the problem using the window of $w_2: t_2, \dots, t_2 + w$ we get the momentary efficiency coefficients $h^{t_2}(X_i^{t_2}, Y_i^{t_2}), h^{t_2+1}(X_i^{t_2+1}, Y_i^{t_2+1}), \dots, h^{t_2+w}(X_i^{t_2+w}, Y_i^{t_2+w})$.

Moving the window continues until $t=T-w+1$, and, as a result of that, for each $DMU_i^{t_j}$, except for $DMU_i^{t_1}$ and $DMU_i^{t_T}$, multiple momentary efficiency coefficients

are calculated using different windows. Thus, $DMU_i^{t_2}$ corresponds to two momentary efficiency coefficients $h_{w_1}^{t_2}$ and $h_{w_2}^{t_2}$, $DMU_i^{t_3}$ to three: $h_{w_1}^{t_3}$, $h_{w_2}^{t_3}$ and $h_{w_3}^{t_3}$, etc. The final value of the momentary efficiency coefficient is the arithmetic mean for various windows:

$$h_{avr}^t = 1/q \sum_{j=1}^q h_{w_q}^t, \quad (4)$$

where q is the number of windows for which momentary efficiency coefficients have been calculated.

When solving problems of comparative evaluations for energy and ecology efficiency of DMUs, one often assumes that they use very similar production technologies (Wang et al., 2013). Then, the differences in efficiency of researched objects can be completely explained by management quality. This assumption places some restrictions on the window method, since production technologies can change overtime. Therefore, the window width should be sufficiently small to avoid comparing objects that use old technologies with objects that use newer and more efficient ones. Most researches that follow this assumption of unchanging production technologies, the value of 3 years is taken as the window width (Wang et al., 2013; Wu et al., 2014). However, in the problem of comparing ecologic and economic efficiencies of regional economic systems, this limitation is insignificant. We are interested in any change of ecologic or economic efficiency of a region, regardless of whether it's caused by improved management, new technologies, environmental protection measures, or a change in regional economy system or energy system structure (Ratner and Nizhegorodtsev, 2017).

Another oft-discussed limitation of the window method is the stability of resulting efficiency coefficient evaluations. Some works, e.g. (Sueyoshi, 1992), suggest to use standard deviation to determine stability:

$$STD_i = \sqrt{\frac{\sum_{t=t_1}^T \sum_{k=1}^{T-w+1} (h_{i,w_k}^t - h_{avr}^t)^2}{w \times (T - w + 1)}} \quad (5)$$

Or, alternatively, the variation:

$$Var_i = \max(h_{i,w}^t) - \min(h_{i,w}^t) \quad (6)$$

Other authors, e.g. (Wu et al., 2014), use the range of efficiency coefficient values for different windows for each moment $t \in (t_1, \dots, T)$:

$$CR_i^t = \max(h_{i,w}^t) - \min(h_{i,w}^t) \quad (7)$$

Regardless of whether one uses the eq. (5), (6) or (7), the stability evaluation for the initial and final moments (t_1 and T) uses only a single value. For this reason, most authors simply omit these moments from their research and evaluate stability only within the research interval (Wang et al., 2013; Wu et al., 2014). This limitation can be overcome by using the “round robin” method, suggested by (Sueyoshi, 1992). The idea behind this method is that efficiency of each DMU is evaluated first only for t_1 , then for (t_1, t_2) , (t_1, t_2, t_3) and so on until (t_1, \dots, T) . This approach allows to obtain a better understanding of the dynamics of each DMU, including the issues of stability and presence of trends, however, this greatly increases the computational complexity of the problem.

Let us look at some advantages and disadvantages of the above-described methods for solving dynamic ecologic and economic efficiency evaluation problems for regional economic systems, using the Southern and North Caucasus Federal Districts during the period of 2010–2014 as an example.

3. RESULTS AND DISCUSSION

We describe each regional economic system with the following set of inputs and outputs:

- x_{1i}^t – annual volume of pollution emitted into atmosphere from stationary sources (thousands of tons),
- x_{2i}^t – annual volume of pollution emitted into atmosphere from automobile transportation (thousands of tons),
- x_{3i}^t – annual volume of unfiltered wastewater discharge (millions of cubic meters),
- x_{4i}^t – annual volume of insufficiently filtered wastewater discharge (millions of cubic meters),
- x_{5i}^t – annual volume of industrial and household waste generation (millions of tons),
- x_{6i}^t – annual volume of fresh water use from surface and underground bodies (millions of cubic meters),
- y_{1i}^t – annual volume of gross regional product in 2010 prices (millions of rubles),
- y_{2i}^t – regional population (thousands of people).

The aforementioned indicators were selected on the one hand due to their logical sufficiency and, on the other hand, due to their availability. Using a representative set of inputs and outputs for modelling ecologic and economic efficiency of regional economic systems allows to analyze more aspects. However, in the event that the amount of used inputs and outputs is close to the amount of DMUs or surpasses that, DEA stops being able to sufficiently discriminate efficiencies (Wang et al., 2013; Wu et al., 2014), which is characterized by an unusually large share of efficient DMUs in the final solution. Therefore, the amount of inputs and outputs should not be excessive, and the inputs and outputs that are selected for use should be informative.

The Russian statistical accounting systems for ecologic aspects of the economy is currently undergoing major improvements. The yearly reports “On the state of environmental protection in Russian Federation” periodically cover the indicators of anthropogenic influence, with the method for their calculation improving over time. These reports can be found on the website of the Ministry of Natural Resources (www.mnr.gov.ru). For instance, the 2010 report differentiates the indicator of wastewater discharge into natural objects and introduces the indicator of regional freshwater consumption, as well as accounts for different methods of garbage disposal (recycling, burying), introduces several climate change indicators, etc. This approach allows to account for a larger number of ecologic indicators, but limits the possible observation periods to those times within which the system remained sufficiently similar.

The suggested set of input and output parameters was chosen based on the results of (Perlis, 2014; Forgione et al., 2016; Ratner & Ratner, 2016; Olejniczak & Lukasik, 2016; Nizhegorodtsev & Ratner, 2016; Verma et al., 2016; Wu et al., 2014). The efficiency coefficient was calculated for each region of the Southern and Northern Caucasus Districts with several methods: the point method, the window method with width equal to the entire observation period, window method with a width of 3 years, and window method with a width of 4 years. Results of the calculations for the point method are presented in Tab. 1, and in Tab. 2 for the window of 3 years.

Tab. 1. Values of ecologic and economic efficiency coefficients of southern Russian regions – calculated with the point method

Region	2010	2011	2012	2013	2014
Adygeya Republic	1	1	1	1	1
Kalmykia Republic	1	1	1	1	1
Krasnodar Region	1	1	1	1	1
Astrakhan Region	1	1	1	1	1
Volgograd Region	1	1	1	1	1
Rostov Region	0.987	1	1	0.988	0.791
Dagestan Republic	1	1	1	1	0.871
Ingushetiya Republic	1	1	1	1	1
Kabardino–Balkar Republic	1	0.864	1	1	0.571
Karatchayevo-Tcherkess Republic	0.801	0.774	0.700	0.630	0.551
Northern Osetiya-Alaniya Republic	0.809	0.858	0.760	0.797	0.473
Tchetchen Republic	1	1	1	1	1
Stavropol Region	0.930	0.848	0.876	0.993	1

Tab. 2. Values of ecologic and economic efficiency coefficients of southern Russian regions – calculated with a window width of 3 years

Region	2010	2011	2012	2013	2014
Adygeya Republic	1	1	1	0.872	1
Kalmykia Republic	1	1	1	1	1
Krasnodar Region	1	1	1	1	1
Astrakhan Region	0.865	0.740	0.898	1	1
Volgograd Region	0.906	1	1	1	1
Rostov Region	0.807	0.893	1	0.968	0.759
Dagestan Republic	1	0.955	1	1	0.756
Ingushetiya Republic	1	1	1	1	1
Kabardino-Balkar Republic	0.705	0.729	1	0.945	0.569
Karatchayevo-Tcherkess Republic	0.680	0.639	0.693	0.597	0.534
Northern Osetiya-Alaniya Republic	0.712	0.761	0.758	0.792	0.473
Tchetchen Republic	1	1	1	1	0.925
Stavropol Region	0.768	0.789	0.835	0.883	0.855

Analyzing the results shown in tables above, we conclude that the ecological and economic efficiency of most southern Russian regions is quite high. The highest efficiency indicators belong to the Adygeya, Kalmykia, Ingushetia and Tchetchen Republics, as well as the Krasnodar region, and the lowest indicators manifest in Karatchayevo-Tcherkess Republic as well as the Northern Osetiya-Alaniya Republic.

As was expected, the window method has a higher discrimination rate due to the fact that the DEA problem is solved for 39 DMUs (for $w=3$) rather than the 13 in the point method. Using the window method, we can see that only three regions of Southern Russia remained effective during the entire observation period: Kalmykia and Ingushetiya republics as well as the Krasnodar region.

To obtain more detailed conclusions we need to perform a comparative analysis of results for individual regions with different window widths ($w = 5, 3, 2$) as well as the point method (fig. 1–2). It's easy to note that using the maximal window width (the entire observation period) leads to minimal coefficient values for non-effective objects, which allows for easier comparison among them.



Fig. 1. Comparing the ecologic and economic efficiency of Karatchayevo-Tcherkess Republic over time with different methods and window widths



Fig. 2. Comparing the results of ecological and economic efficiency of Stavropol region over time with different methods and window widths

Narrower windows lead to higher efficiency coefficients. We would like to note that the direction in which dynamics of DMU efficiency change (i.e. whether they drop or rise) can also differ throughout various methods. For example, analyzing the dynamics of efficiency in the Karachayevo-Tcherkess Republic using the point method, one can notice a decrease. This implies that the efficiency of this republic worsens over time compared to other regions. However, using a window width equal to the observation period will show that there's no particular trend in these dynamics. That is to say, efficiency of the region will sometimes rise and sometimes drop, showing a lack of a coherent ecologic policy in this region. No particular trends show up with window widths of 3 and 2 years for this region either.

Comparing the stability of efficiency evaluations with different window widths (eq. 5), we can point out that the standard deviation for most regions changes insignificantly.

Tab. 3. Standard deviation of evaluations of ecologic and economic efficiency of southern Russian regions with varying window widths

Region	<i>STD, w=5</i>	<i>STD, w=3</i>	<i>STD, w=2</i>
Adygeya Republic	0.0684	0.0564	0.0444
Kalmykia Republic	0.0009	0.0000	0.0000
Krasnodar Region	0.0000	0.0000	0.0000
Astrakhan Region	0.1534	0.1173	0.0777
Volgograd Region	0.0520	0.0314	0.0000
Rostov Region	0.1038	0.0895	0.0823
Dagestan Republic	0.1055	0.0805	0.0836
Ingushetiya Republic	0.0000	0.0000	0.0000
Kabardino-Balkar Republic	0.1881	0.1636	0.1547
Karachayevo-Tcherkess Republic	0.0615	0.0560	0.0789
Northern Osetiya-Alaniya Republic	0.1294	0.0990	0.1154
Tchetchen Republic	0.0333	0.0248	0.0233
Stavropol region	0.0445	0.0424	0.0626

The most stable indicators with varying window widths throughout the entire period are demonstrated by the regions that have the highest efficiency values, as is to be expected. These regions are the Ingushetiya, Kalmykia and Tchetchen Republics, as well as the Krasnodar and Volgograd regions. The most notable changes in stability, depending on window widths, can be observed only in the Astrakhan region and the Northern Osetiya-Alaniya Republic. Therefore, it is difficult to judge which window width is more appropriate for increased stability of the results.

4. CONCLUSIONS

The main result of the paper is the adaptation of the window method to the tasks of monitoring the complex ecological and economic efficiency of the regional production systems dynamically. In contrast to simply solving unrelated problems of estimating the comparative effectiveness of RES at any particular point of time in the research period, the window method allows us to reveal the dynamics of efficiency associated with the shift in the efficiency frontiers of the entire set of DMUs under consideration due to technological eco-innovations (the best available production technologies) or a change in the structure of the region's economics.

Estimates of the ecological and economic efficiency of RES calculated with a window of the maximum width equal to the entire observation period make it possible to discriminate the RES's in the best way.

The simplicity of the technical implementation of the proposed method and the availability of the necessary software for its use allow one to hope for its wide implementation in the practice of regional environmental management.

ACKNOWLEDGMENT

This study is supported financially by the Russian Foundation for Basic Research (RFBR), project No. 16-06-00147 "Development of data envelopment analysis models for optimizing development of regional economic systems based on ecologic parameters".

REFERENCES

- Bian, Y., He, P., & Xu, H. (2013). Estimation of potential energy saving and carbon dioxide emission reduction in China based on an extended non-radial DEA approach. *Energy Policy*, 63, 962–971. doi:10.1016/j.enpol.2013.08.051
- Carrillo, M., & Jorge, J. M. (2016). A multi-objective DEA approach to ranking alternatives. *Expert Systems with Applications*, 50, 130-139. doi:10.1016/j.eswa.2015.12.022
- Charnes, A., Clarke, C., Cooper, W., & Golany, B. (1984). A development study of DEA in measuring the effect of maintenance units in the U.S. Air Force. *Annals of Operation Research*, 2(1), 95–112.
- Cook, W. D., & Seiford, L. M. (2009). Data Envelopment Analysis (DEA) – Thirty years on. *European Journal of Operational Research*, 192, 1–17. doi:10.1016/j.ejor.2008.01.032
- Fare, R., Grosskopf, S., & Lovell, C. A. K. (1994). *Production Frontiers*. Cambridge University Press.
- Färe, R., & Grosskopf, S. (2004). Modelling undesirable factors in efficiency evaluation: comment. *European Journal of Operational Research*, 157(1), 242–245. doi:10.1016/S0377-2217(03)00191-7
- Forgione, H., Pregitzer, C., Charlop-Powers, S., & Gunther, B. (2016). Advancing urban ecosystem governance in New York City: Shifting towards a unified perspective for conservation management. *Environmental Science & Policy*, 62, 127–132. doi: 10.1016/j.envsci.2016.02.012

- Khrustalev, E. Yu., & Ratner, P. D. (2015a). Analysis of ecological efficiency of Russia's electric energy companies through the data envelopment analysis methodology. *Economic Analysis: The Theory and Practice*, 35, 33–42.
- Khrustalev, E. Yu., & Ratner, P. D. (2015b). Eco-innovations in energy generation industry: the assessment of comparative effectiveness. *Innovations*, 9, 8–14.
- Korhonen, P. J., & Luptacik, M. (2004). Eco-efficiency analysis of power plants: An extension of data envelopment analysis. *European Journal of Operational Research*, 154(2), 437–446. doi:10.1016/S0377-2217(03)00180-2
- Melnikov, R. M. (2016). Development of a methodology for assessing the effectiveness of scientific and innovative programs taking into account foreign experience. *Innovations*, 10, 65–73.
- Malmquist, S. (1953). Index numbers and indifference surfaces. *Trabajos de Estadística*, 4, 209–242.
- Nizhegorodtsev, R. M., & Ratner, S. V. (2016). Trends in the development of industrially assimilated renewable energy: the problem of resource restrictions. *Thermal Engineering*, 63(3), 197–207. doi: 10.1134/S0040601516030083
- Olejniczak, K., & Lukasik, K. (2016). Building Ecological Organizational Culture in the Modern Enterprise – Case of Henkel. *International Journal of Contemporary Management*, 15(1), 33–47. doi: 10.4467/24498939IJCM.16.002.4835
- Perlis, M. L. (2014). The Climate and Energy Policy Basis for EPA's First-Ever CO2 Emission Standards for Power Plants. *The Electricity Journal*, 27(3), 35–44. doi:10.1016/j.tej.2014.03.005
- Ratner, S. V. (2016). Problems of optimizing the trajectories of the development of regional socio-economical systems on ecological parameters. *Drukerovsky Bulletin*, 2, 30–41.
- Ratner, S. V., & Ratner, P. D. (2016). Regional Energy Efficiency Programs in Russia: The Factors of Success. *Region*, 3(1), 68–85. doi:10.18335/region.v3i1.71
- Ratner, S. V., & Nizhegorodtsev, R. M. (2017). Analysis of renewable energy projects' implementation in Russia. *Thermal Engineering*, 64(6), 429–436. doi:10.1134/S0040601517060052
- Verma, R. L., Borongan, G., & Memon, M. (2016). Municipal Solid Waste Management in Ho Chi Minh City, Vietnam. Current Practices and Future Recommendation. *Procedia Environmental Sciences*, 35, 127–139. doi: 10.1016/j.proenv.2016.07.059
- Wang, K., Shiwei, Y. U., & Zhang, W. (2013). China's regional energy and environmental efficiency: A DEA window analysis based dynamic evaluation. *Mathematical and Computer Modelling*, 58(5-6), 1117–1127. doi:10.1016/j.mcm.2011.11.067
- Wu, H., Shi, Y., & Zhu, W. (2014). Effectiveness of the policy of circular economy in China: A DEA-based analysis for the period of 11th five-year-plan. *Resources, Conservation and Recycling*, 83, 163–175. doi:10.1016/j.resconrec.2013.10.003

matching pursuit, bearing faults, energy error

Kamil JONAK*, Paweł KRUKOW**

MATCHING PURSUIT ALGORITHM IN ASSESSING THE STATE OF ROLLING BEARINGS

Abstract

In this paper the results of Matching Pursuit (MP) Octave algorithm applied to noise, vibration and harness (NVH) diagnosis of rolling bearings are presented. For this purpose two bearings in different condition state were examined. The object of the analysis was to calculate and present which energy error values of MP algorithm give the most accuracy results for different changes in bearing structures and also how energy values spread in time-frequency domain for chosen energy error value.

1. INTRODUCTION

With the development of industry and the entry of a vast number of everyday devices containing from a few to dozens of moving parts, the need for production and installation of bearings significantly increased. Although the technology of bearings is improving from year to year, it is not possible to produce a reliable bearing, not liable to damage in an infinitely long time. The operation of the bearing greatly reduces its operating life. To avoid the costs generated by the device closed to traffic due to damage to the bearings began to use a wide range of diagnostic tools enable ongoing assessment of its condition. By using diagnostic methods it can be early detection of bearing damage and its replacement at a convenient time for the user (Cempel, 1989).

* Lublin University of Technology, Nadbystrzycka 36, 20-618 Lublin, k.jonak@pollub.pl

** Medical University of Lublin, Głuska 2, 20-439 Lublin, pawel.krukow@umlub.pl

One of the most commonly used methods of diagnosis of bearings is the study of NVH (Nguyen-Schafer, 2016). Vibro-acoustic measurements are based on the study of dynamic noise generated by operating machines or their components. With the development of computer analysis vibro-acoustic techniques became much more accurate and the time required for a complete analysis of a single item decreased significantly. In the case of a diagnosis of bearings, studied interference dynamic vibration components are working bearings. The main reason for using this method for diagnostics of the bearing is its non-invasive examination of their condition and the possibility of accurate detection of the type of damage occurring.

There are many methods of signal analysis which can be implemented to estimate the working bearing condition. For the most precise analysis of bearing state Time-frequency signal analysis method will be the best due to fact that this kind of analysis shows both time and the frequency domain. As vibration signals are non-stationary, the Time-frequency analysis features are very useful tools to describe processes that occur in the bearing (Gao & Yan, 2011). For many years to monitor machinery condition people have been using Windowed Fourier Transform (WFT) and Short Time Fourier Transform (STFT), but those algorithms show weak performance. To improve time resolution of STFT analysis the Continuous Wavelet Transform (CWT) was developed (Chandra & Sekhar, 2016; Yan, Gao & Chen, 2014). The main disadvantage of CWT is that the algorithm needs a lot of time to be implemented. Matching Pursuit (MP) is the next step in algorithm quality improvement (Chandran et al., 2016). The main difference between MP and CWT is that MP uses a package of wavelets, called wavelet dictionaries compared to a single wave form in CWT, which allows to perform better analysis of vibration signals. Thanks to using wavelet dictionaries, the results of Time-frequency analysis show the best time resolution from among the rest of Time-frequency algorithms. For many recent years Matching Pursuit algorithm has frequently been used for fault detection in rolling bearings (Liu, Ling & Gribonval, 2002). In that time many of MP features were upgraded or changed (Tang et al., 2012). Some of them proposed to use impulse dictionaries (Cui, Wang & Lee, 2014), which provide higher efficiency and better stability. In a paper by He (2016), the dictionary applied for diagnostics was over-completed, which gives a low signal to noise ratio values for large rolling elements sliding. In many other papers (Cui, Gong, Zhang & Wang, 2016) changes involving the MP algorithm were focused on dictionary (Cui et al., 2016).

The main goal of this paper is an implementation of an MP algorithm based on an Octave dictionary (Kuś, Róžański & Durka, 2013) for bearings fault diagnosis. The main differences between traditional dictionaries and the Octave dictionary is an ability to control maximum error in every single MP iteration. With the ability to use error control there is a possibility to choose the appropriate size of dictionary redundancy when the energy error value is being

decreased, the size of the dictionary increases. Constant MP energy value error will not have any impact on atoms' location, so the energy density distribution will not be incorrect in different signal parts. Thanks to an appropriate selection of the dictionary size, MP decomposition will take less time and will be more accurate, which will have significant impact on diagnostic results.

2. MATCHING PURSUIT ANALYSIS

MP is algorithm based on an iterative decomposition of a signal by waveforms called atoms (g_n) (Mallat & Zhang, 1993). Atoms in the Time-frequency domain can be obtained from modulation, translation and scaling of a single window function:

$$g_{\gamma}(t) = \frac{1}{\sqrt{s}} g\left(\frac{t-u}{s}\right) e^{i\xi\omega t} \quad (1)$$

where: u – translation,
 s – duration,
 ω – modulation,
 ξ – frequency,
 γ – set of parameters $\{u, \omega, s, \phi\}$.

>Atom functions are usually modulated Gaussians so they can be called “Gabor Atoms” (GA) and can be defined:

$$g_{\gamma}(t) = K(\gamma, \phi) e^{-\pi \left(\frac{t-u}{s}\right)^2} \sin(\omega(t-u) + \phi) \quad (2)$$

where: $K(\gamma, \phi)$ – is normalization of $\|g_{\gamma, \phi}\| = 1$,

A large number of GA creates a dictionary of waveforms described as $D = \{g_1, g_2, \dots, g_n\}$ where $\|g_i\| = 1$, which allows to start the iteration procedure. The first iteration step chose atom g_{γ_0} which values describe signal parameters accurately (Durka, Ircha & Blinowska, 2001). In the next steps other atoms will be matched to signal residuum, R^n s which will remain after the values of the previous iteration will be cut off.

$$\begin{cases} R^0 s = s; \\ R^n s = \langle R^n s, g_{\gamma_n} \rangle g_{\gamma_n} + R^{n+1}; \\ g_{\gamma_n} = \arg \max_{g_{\gamma_i} \in D} |\langle R^n s, g_{\gamma_i} \rangle| \end{cases} \quad (3)$$

As mentioned in the introduction, Octave dictionary has a unique option of energy error control, which can be changed at the beginning of the dictionary construction task.

Energy error (ε) will correspond to (Kuś, Różański & Durka, 2013):

$$\begin{aligned} d(g_{(s,\omega,u,\phi)}, g_{(as,\omega,u,\phi)}) &\leq \varepsilon \\ d(g_{(s,\omega,u,\phi)}, g_{(as,\omega+\Delta\omega,u,\phi)}) &\leq \varepsilon \\ d(g_{(s,\omega,u,\phi)}, g_{(as,\omega,u+\Delta u,\phi)}) &\leq \varepsilon \end{aligned} \quad (4)$$

The final result of MP is Time-frequency spectrogram (Fig. 1). The spectrogram shows signal energy distribution in the Time-frequency domain. Signal energy was obtained by the use of Wigner distribution for one g_γ in combination with conservation of MP energy:

$$\int_{-\infty}^{+\infty} \int_{-\infty}^{+\infty} Es(t, \omega) dt d\omega = \|s\|^2 \quad (5)$$

where: $Es(t, \omega)$ – translation,
s – Signal energy density.

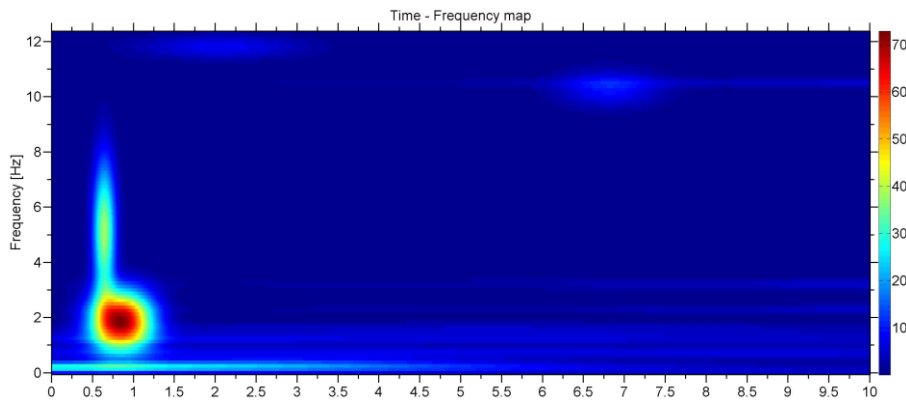


Fig. 1. Time-frequency spectrogram with energy density distribution – atom placed in bottom left corner represents biggest concentration of energy (red color)

3. EXPERIMENT

Researches were conducted on a test stand (Fig. 2) equipped with AC motor, jaw coupling and a shaft with two bearings and one of them was the test bearing. In this setup a magnetic break placed at the end of the shaft with breaking torque 1–10Nm was a load. An accelerometer, Brüel&Kjaer nr.4394, is a miniature device created for shock and vibration measurement with frequency range 1–25000Hz. The accelerometer was placed on the bearing case and connected to a signal amplifier PCB Model 482A20. A National Instruments PXI-1044 computer equipped with NI PXI-4472B data acquisition card was used to convert analogue signals to digital signals. For data acquisition LabVIEW was used. Sampling frequency was set at 20 KHz. Signal analyses were done in Matlab.

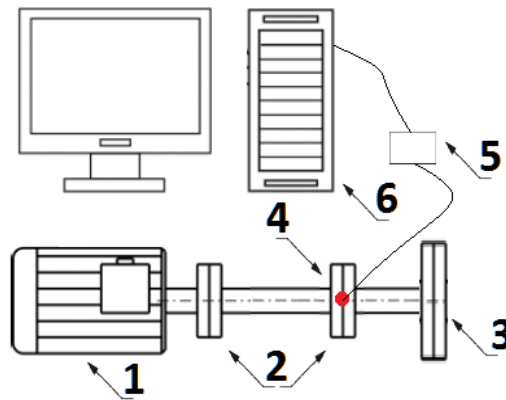
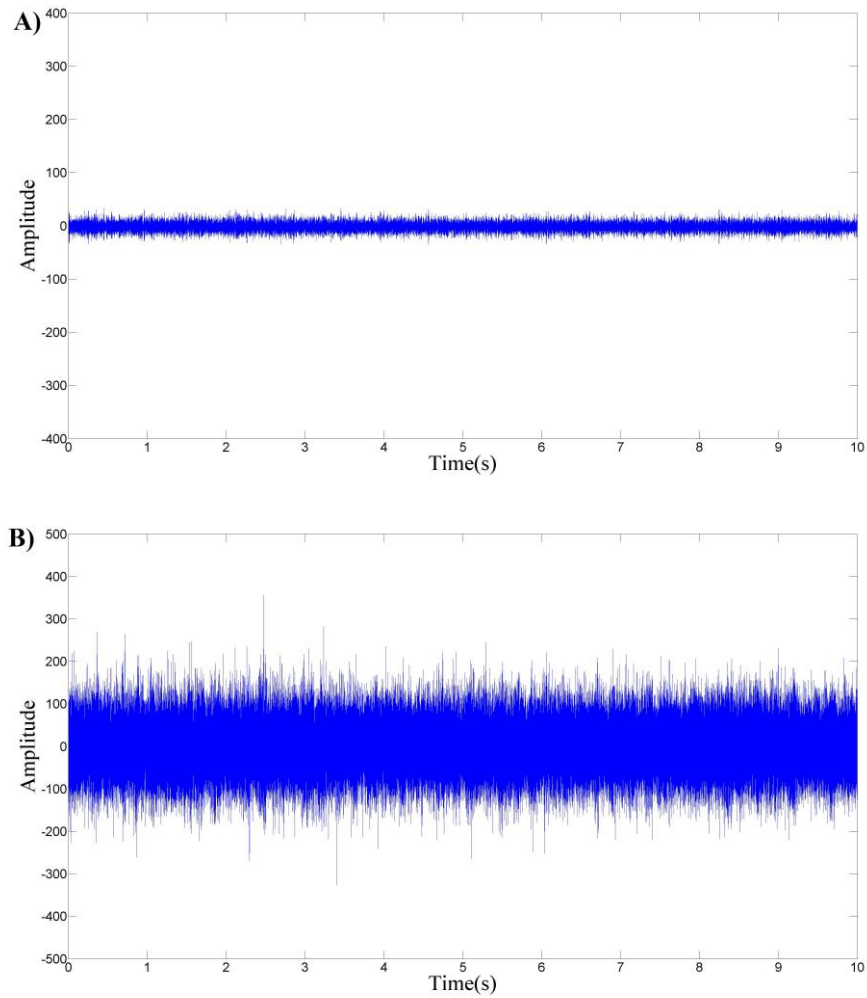


Fig. 2. Test Stand: 1 – AC Motor, 2 – Bearings, 3 – Magnetic break, 4 – Accelerometer, 5 – Amplifier, 6 – Computer

4. RESULTS

In order to verify the usefulness of MP algorithm based on Octave dictionary in rolling bearing fault detection, two bearings in different wear conditions were tested. As presented in Fig.2 bearings worked in pairs, to avoid propagation of oscillations from the damaged bearing to the healthy one, after one measurement cycle the damaged bearing that worked under an accelerometer was switched with the health one. Time duration of one measurement cycle was set into 10s. During the whole cycle velocity was constant at 100Hz. The next set of data collected from the experiment was analyzed by an MP algorithm with Octave dictionary. To show energy distributions in signals precisely the number of iterations was set into 20 for all cases.

Raw signals acquired from the experiment are presented as (Fig. 3) time-amplitude plots. The first graph (A) presents the signal registered for a bearing in normal condition state. The second graph (B) presents the recording for a bearing with a rolling element fault (REF).



**Fig. 3. Raw signal of bearing vibrations under conditions:
A) Health condition B) Rolling element fault**

Analyzing amplitude values on both plots it can be seen that a bearing in health state (A) has lower amplitude values in comparison to amplitude values from a damaged bearing (B).

After gathering the data was processed by an MP algorithm. The first step of the MP analysis was to select 25 appropriate signal episodes for future decomposition. Due to long calculation time for small energy error values and to illustrate differences between single reconstruction function, the analyzed time was set up for 0.16s. Octave dictionary implemented to analysis was constructed separately for three energy error values 0.1, 0.01 and 0.001. Averaged Matching Pursuit coefficients from 25 segments were placed in Tab.1 for the health state bearing and in Tab.2 for bearing with REF. Values are presented according to iterations “I” and energy error values “ER”. The number of Gabor atoms for each error value are presented in the “A” row. Energy values are placed in “E” rows separately for different energy error values (E1, E2, E3). Individual differences (in percent) between energy values for different energy errors were placed in C1 as E1–E2 difference and C2 as E2–E3 difference.

Tab. 1. Matching Pursuit coefficients for HC bearing.
ER – energy error value; A – Number of functions in
dictionary (in millions); I – iteration; E(1,2,3) – energy
value for single Gabor Atom; C1 – percentage difference
between E1 and E2; C2 – percentage difference between
E2 and E3

ER	0.1	0.01	0.001		
A	114	4.008	128.009	C1	C2
I	E1	E2	E3	%	%
0	196	220.1	220.7	12.29	0.27
1	139	141.4	141.5	1.70	0.10
2	124	123.5	123.1	0.44	0.27
3	115	118.1	118.1	2.68	0.04
4	114	107.1	106.9	6.02	0.20
5	106	94.2	97.5	11.13	3.47
6	77	80.9	81.3	5.12	0.48
7	75	79.7	79.8	6.24	0.13
8	72	73.4	73.3	1.94	0.13
9	70	55.1	54.6	21.33	0.85

Tab. 2. Matching Pursuit coefficients for REF bearing.
ER – energy error value; **A** – Number of functions in dictionary (in millions); **I** – iteration; **E(1,2,3)** – energy value for single Gabor Atom; **C1** – percentage difference between E1 and E2; **C2** – percentage difference between E2 and E3

ER	0.1	0.01	0.001		
A	114	4.008	128.009	C1	C2
I	E1	E2	E3	%	%
0	694.96	781.24	783.57	12.42	0,30
1	518.66	531.14	532.08	2.41	0.18
2	511.43	513.97	514.21	0.50	0.05
3	488.49	495.91	497.08	1.52	0.24
4	340.33	382.31	382.91	12.33	0.16
5	339.90	369.38	369.99	8.67	0.17
6	334.33	362.01	362.46	8.28	0.12
7	334.23	349.63	350.28	4.61	0.19
8	324.58	326.87	327.71	0.70	0.26
9	314.03	321.18	321.54	2.28	0.11

Analyzing results presented in table one and two, it can be seen that the biggest differences in energy values are between E1 and E2 energy error values and even a different bearing state does not affect the results. According to the results it can be said that the highest accuracy with good calculation time (bigger dictionary size affects calculation time) has 0.01 energy error value. Energy values for the REF bearing are higher in every energy error case in comparison to HC which is normal for this bearing fault.

The last step of the analysis was the creation of an MP spectrogram to demonstrate the arrangement of Gabor atoms in the time-frequency system. Both spectrograms presented MP decomposition results for 0.01 energy error and correspond to results presented in tables 1 and 2.

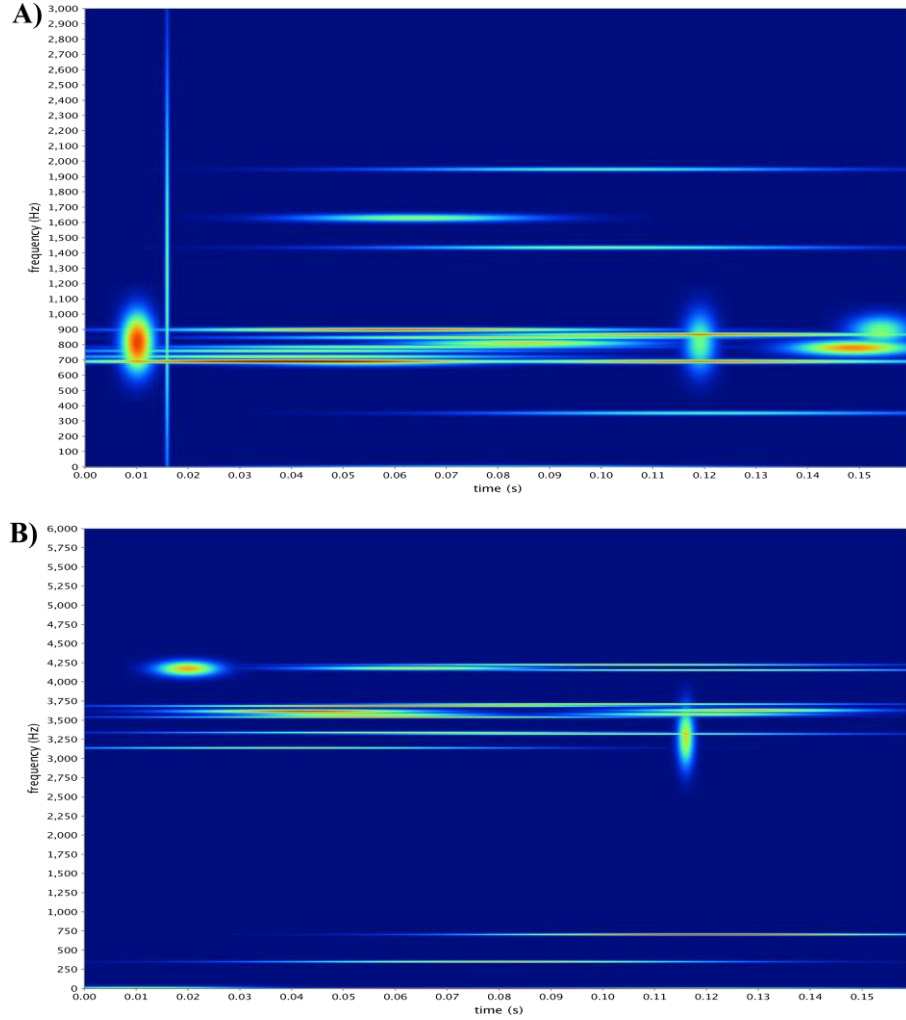


Fig. 4. Matching Pursuit results: A) Health condition B) Rolling ele. fault

For the HC (Fig. 4A) bearing Gabor atoms were localized mostly at 600–1000Hz frequency band, through almost the whole time. The second spectrogram (B) contains energy values for REF bearing. In this case very high energy values were concentrated at 3K–4K Hz and some under the 1 kHz frequency band.

5. CONCLUSIONS

In this paper the results of the application of an MP algorithm with Octave dictionary for the diagnostics of the bearing condition are presented. Implementation of Octave dictionary provided an opportunity to choose an energy error value which is the most proper for the analyzed conditions. The results show that for bearing state diagnosis the best energy error value is 0.01 due to good energy value representation with decent Gabor atom quantity. Thanks to the balanced algorithm structure, energy values can easily show abnormalities contained in signals with good accuracy and decent calculation time. To show differences in frequency bands between the examined bearings, the spectrograms of signal energy density distribution had been created. As the spectrograms show, Gabor atoms' locations in time-frequency domain can be compared with characteristic estimates of different bearing faults. The coefficients acquired as the results of the MP algorithm show direct differences in energy level for each iteration according to bearing condition state. For future analysis regulation of energy error estimator values would be the best method for preposition the data to fed Machine Learning algorithms.

REFERENCES

- Cempel, C. (1989). *Wibroakustyka Stosowana*. Warszawa: PWN.
- Chandra, H. N., & Sekhar, A. S. (2016). Fault detection in rotor bearing systems using time frequency techniques. *Mechanical Systems and Signal Processing*, 72–73, 105–133. doi: dx.doi.org/10.1016/j.ymssp.2015.11.013
- Chandran, S., Mishra, A., Shirhatti, V., & Ray, S. (2016). Comparison of Matching Pursuit Algorithm with Other Signal Processing Techniques for Computation of the Time-Frequency Power Spectrum of Brain Signals. *The Journal of Neuroscience*, 36(12), 3399–3408. doi: 10.1523/JNEUROSCI.3633-15.2016
- Cui, L., Wu, N., Ma, C., & Wang, H. (2016). Quantitative fault analysis of roller bearings based on a novel matching pursuit method with a new step-impulse dictionary. *Mechanical Systems and Signal Processing*, 68–69, 34–43. doi: dx.doi.org/10.1016/j.ymssp.2015.05.032
- Cui, L., Gong, X., Zhang, J., & Wang, H. (2016). Double-dictionary matching pursuit for fault extent evaluation of rolling bearing based on the Lempel-Ziv complexity. *Journal of Sound and Vibration*, 385, 372–388. doi: dx.doi.org/10.1016/j.jsv.2016.09.008
- Cui, L., Wang, J., & Lee, S. (2014). Matching pursuit of and adaptive impulse dictionary for bearing fault diagnosis. *Journal of Sound and Vibration*, 333, 2840–2862. doi: dx.doi.org/10.1016/j.jsv.2013.12.029
- Durka, P. J., Ircha, M., & Blinowska, K. J. (2001). Stochastic Time-Frequency Dictionaries for Matching Pursuit. *IEEE Transactions of Signal Processing*, 49, 507–510. doi: 10.1109/78.905866
- Gao, R. X., & Yan, R. (2011). *Wavelets: Theory and Applications for Manufacturing*. Springer. doi: DOI 10.1007/978-1-4419-1545-0_2
- He, G., Ding, K., & Lin, H. (2016). Fault feature of rolling element bearings using sparse representation. *Journal of Sound and Vibration*, 366, 514–527. doi: dx.doi.org/10.1016/j.jsv.2015.12.020

- Kuś, R., Róžański, P. T., & Durka, P. J. (2013). Multivariate matching pursuit in optimal Gabor dictionaries: theory and software with interface for EEG/MEG via Svarog. *Biomedical Engineering Online*, 12, 1-28. doi: 10.1186/1475-925X-12-94
- Liu, B., Ling, S. F., & Gribonval, R. (2002). Bearing failure detection using matching pursuit. *NDT&E International*, 35, 255–262.
- Mallat, S., & Zhang, Z. (1993). Matching pursuit with time-frequency dictionaries. *IEEE Trans On Signal Processing*, 41, 3397–3415. doi: 10.1109/78.258082
- Nguyen-Schafer, H. (2016). *Computational Design of Rolling Bearings*. Springer. doi: 10.1007/978-3-319-27131-6
- Tang, H. F., Chen, J., & Dong, G. M. (2012). Signal complexity analysis for fault diagnosis of rolling element bearing based on matching pursuit. *Journal of Vibration and Control*, 18, 671–683. doi: 10.1177/1077546311405369
- Yan, R., Gao, R. X., & Chen, X. (2014). Wavelets for fault diagnosis of rotary machines: A review with applications. *Signal Processing*, 96, 1–15. doi: 10.1016/j.sigpro.2013.04.015

computer model, simulation experiment, multi-criteria assessment

Sławomir KUKLA*, Marek SMETANA**

A SIMULATION EXPERIMENT AND MULTI-CRITERIA ASSESSMENT OF MANUFACTURING PROCESS FLOW VARIANTS TESTED ON A COMPUTER MODEL

Summary

The article presents issues relating to designing and improvement of manufacturing processes based on a modelling and simulation method. The 3D model of a production line has been designed and simulation experiment, conducted on the Arena model prepared in a versatile package for modelling and simulation of manufacturing systems and representing functioning of the system, has been carried out. The results obtained from the experiment and analyses of time and ergonomics of work at a work station were subject to multi-criteria assessment based on a point-by-point method of assessment according to Yager.

1. INTRODUCTION

In the face of heavy competition and faster and faster changes in the labour market, companies strive to achieve the shortest possible time to commence sale of products that suit exact customer requirements. Shortening the production cycle, while maintaining the minimum time and cost, proper quality, safety and ergonomics of work, as well as environmental guidelines, has caused the necessity of introducing changes in designing and management of processes. Functioning on the concept of lean manufacturing, the enterprise assumes the use of a number of tools for continuous improvement. They can be applied

* Department of Production Engineering, University of Bielsko-Biala, ul. Willowa 2, 43-309 Bielsko-Biala, 33 8279 253, skukla@ath.bielsko.pl

** Department of Civil Protection, Faculty of Safety Engineering, VŠB – Technical University of Ostrava, 597 322 820, marek.smetana@vsb.cz

as an aid to research the causes of problems, analysis of processes, creating improvement ideas and determining their impact on functioning of the manufacturing systems (Dennis, 2016; Manas, 2015).

Development of information systems has become an opportunity to optimize preparation of production, among others, through the use of modelling and simulation tools.

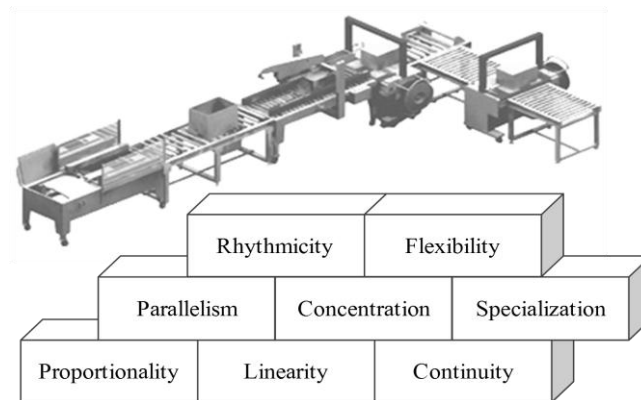


Fig. 1. The principles of organizing production cells
(own study based on Pisz, Sęk& Zielecki, 2013)

There are various principles being guidelines at organization and improvement of production cells (Fig. 1):

- the principle of proportionality that points to the necessity of distribution of production tasks in such a way that all work stations, production cells and operation performed on them were adjusted to one another in terms of production capacity, as well as to prevent internal distributions,
- the principle of linearity that emphasises unidirectionality of the process flow during realization of a part of the production process, i.e. flow paths of the subjects of labour between successive operations should be as short as possible,
- the principle of continuity that recommends eliminating all gaps of the manufacturing process which can have a negative influence on shaping economic as well as production and organizational parameters,
- the principle of parallelism: it is based on manufacturing different products at the same time in order to shorten the production cycle,
- the principle of concentration: it recommends focusing production factors in a particular production area which results in a higher level of their use,
- the principle of specialisation that assumes reducing the diversity of production tasks and range of products to facilitate planning and organization of the manufacturing process, as well as to increase the performance,

- the principle of rhythmicity relating to the problem of production in a specific rhythm resulting in regular occurrence of the same phenomena in a time interval,
- the principle of flexibility that puts emphasis on such designing of the manufacturing process, as to easily adapt it to new conditions (Pisz, Sęk & Zielecki, 2013; Sobaszek & Gola, 2015).

2. MODELLING AND SIMULATION OF MANUFACTURING SYSTEMS

A model means simplified object whose degree of similarity in comparison with a modelled object causes that the research carried out on it provides significant and useful information in terms of the purpose of research.

Simulation is a technique used to analyse a real system based on a computer model that represents it. Simulation of systems is understood as the action of presenting a real system with the use of a symbolic model, which can be easily operated and provides numeric results (Dima& Man,2015; Rossetti, 2016).Simulation methods are used more and more often to solve problems in the area of preparation and organization of manufacturing. The use of the modelling and simulation of manufacturing systems method is based on creating a computer model of a real condition, or designing a process and carrying out a number of simulation tests on it (Fig. 2). On the basis of the reports obtained, it is possible to analyse parameters of the systems and create improvement proposals (Kelton, Sadowski & Sturrock, 2007; Kłos, Patalas-Maliszewska & Trebuna, 2016, Maciąg, Piertróń & Kukla, 2013; Rainey & Tolk, 2015).

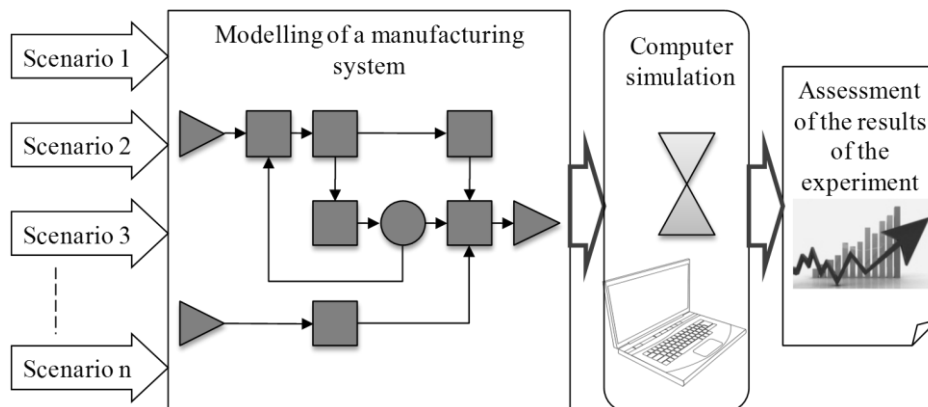


Fig. 2. Modelling and simulation of manufacturing systems

The main objectives of simulation models are as follows:

- supporting manufacturing decisions making,
- presenting features and parameters of the system that has not been known so far.

Using tools for modelling and simulations generates numerous benefits for the enterprise:

- the possibility to observe the course of the processes analysed in changed conditions, such as changes in terms of machinery park, transport organization, cooperation, modified flow of information, etc.,
- examination and assessment of parameters of the systems before launching it in real conditions,
- the possibility to determine the length of the production cycle,
- identifying parameters having significant impact on the economic result of the enterprise,
- determining possible hazards in terms of flow of information, organization of logistics and manufacturing processes,
- determining the risk of different variants in a situation of absence of experience as well as limited knowledge about the process investigated. however, simulation methods have a lot of vices:
- time consumption of constructing a model,
- no guarantee of finding the optimal solution,
- the need of having wide knowledge of the analysed system by the author of a model,
- the need of fluency in simulation software,
- test results that are difficult to interpret,
- problematic transfer of test results to other tested objects,
- profitability in case of high series and mass production (Maciąg, Piotroń & Kukla, 2013; Plinta, 2015).

3. MULTI-CRITERIA ASSESSMENT OF VARIANTS

As a result of a simulation experiment, the set of reports is obtained. The reports cover the results associated with performance, use of resources, queues, delays, lead time of production tasks, costs, etc. It is difficult to clearly evaluate the results of the experiment, especially when considering several evaluation criteria. Commonly known multi-criteria assessment methods might be helpful (Fig. 3). One of the examples is a multi-criteria point-by-point assessment according to Yager that is based on Saaty's matrices. Selecting one of the variants with the use of Yager's method starts with determining input data including: number of criteria (m), number of variants (n), number of experts (p) and determining the scale of grades and criteria (Kukla, 2014).

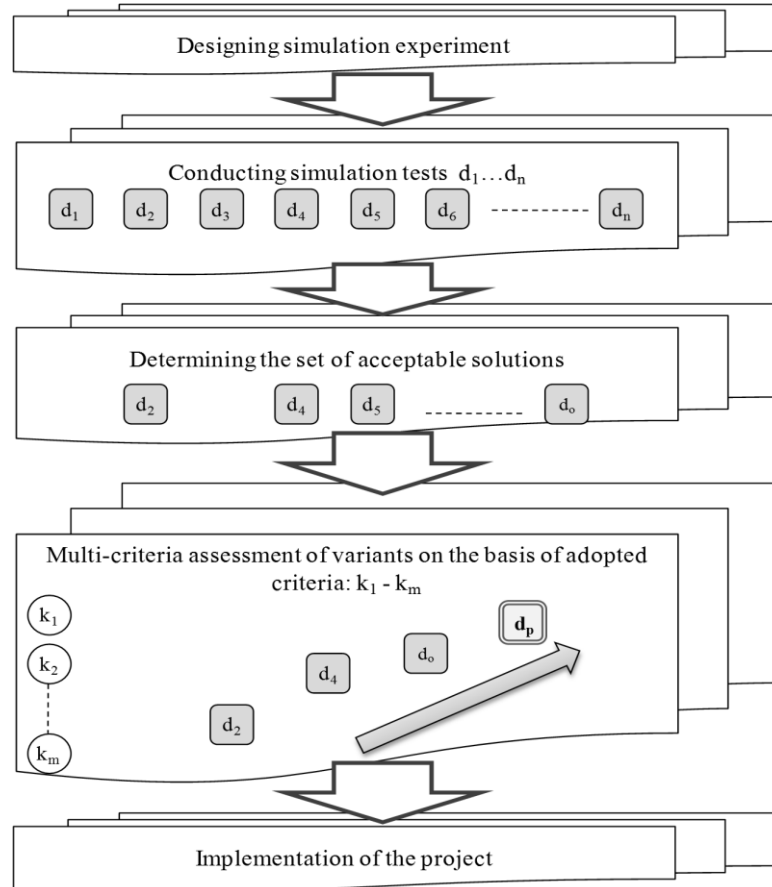


Fig. 3. Simulation experiment and multi-criteria assessment of variants

At the beginning, the criteria are compared in pairs, an overall matrix of assessment is created and weights of criteria are set with the use of the power method. In a further step, based on the results of the experiment and analyses conducted, individual variants of solutions are assessed in relation to each of the criteria and in line with a point-by-point scale adopted. Then, upon summarizing partial grades, normalised grades and overall normalised grades are created on the basis of them by aggregating normalised grades of individual experts for each of the variants, considering evaluation criteria adopted. Normalised decisions are calculated by raising the total normalised values to powers equal to the weights of criteria. For each of the variants, the lowest grade, among all the obtained, for subsequent criteria is selected. A variant, to which the highest grade corresponds (a component of optimum decision) is the most advantageous variant in the light of adopted assessment criteria (Kukla, 2014; Kukla, 2016).

4. A DESCRIPTION OF THE RESULTS OBTAINED

The object of research in the study was the production line associated with the food industry. The purpose of the research was to design a new line based on machinery and equipment of the line already functioning in the plant.

The 3D models of the production line were designed with the use of the Autodesk Inventor software. Measurement of available production space and line equipment was taken and a computer model to visualize the work station being designed was created. Then a simulation model of the line was constructed in the Arena package (Fig. 4). Upon testing the model, a simulation experiment was designed for three variants of solutions.

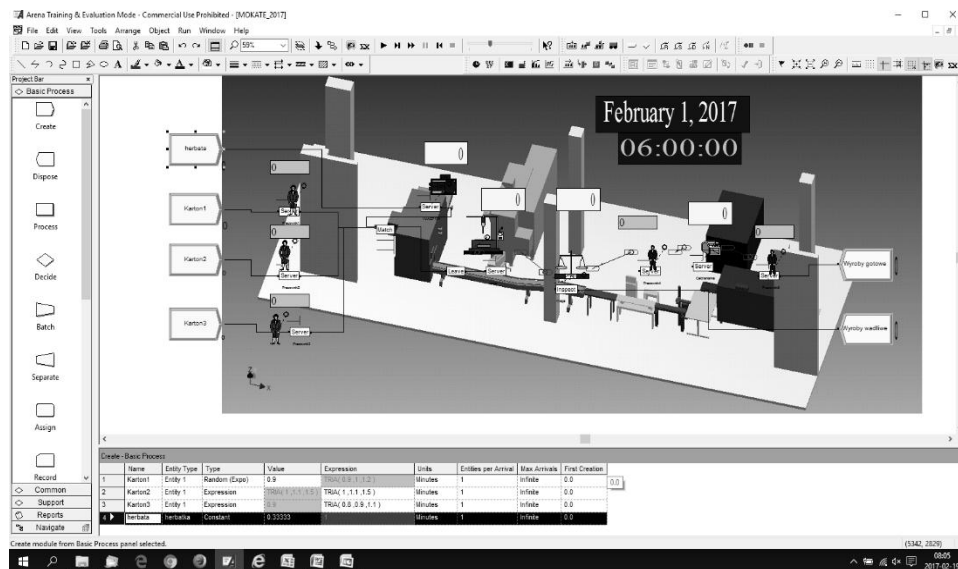


Fig. 4. Simulation model in the Arena software

Thanks to visualisation of work at the work station and observation of working conditions at similar work stations in the plant, an ergonomic analysis of work at given work stands was carried out. The ergonomic analysis was carried out with the use of the point-by-point method, while hand machining was divided into procedures. The aim was to improve the work station in order to eliminate actions that are unnecessary and uncomfortable for an employee.

The assessment of ergonomics of work on the line was carried out on the basis of the chart of ergonomic positions, taking into account 9 situations at the work station (Falzon, 2015; Kukla, 2016). Number grades were assigned to each action and position at work, which correspond to three zones of a three-stage scale (Fig. 5).

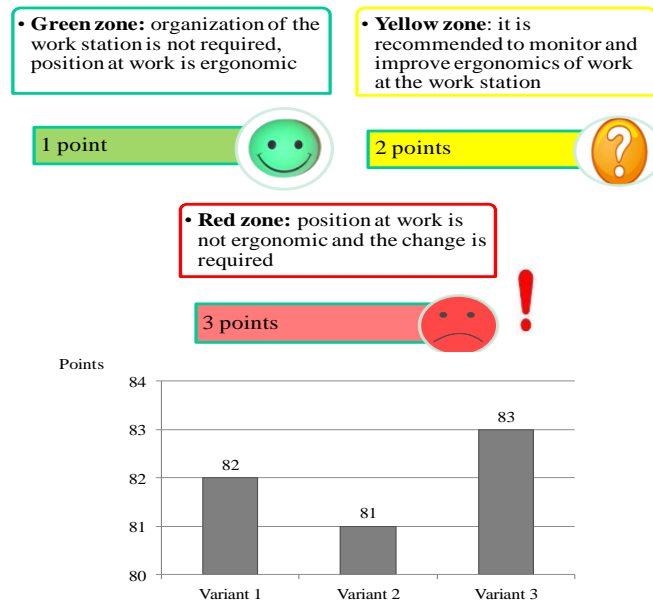


Fig. 5. Point-by-point assessment of ergonomics of work at a work station

On the basis of the 3D model, distance covered by the products on the production line was specified (Fig. 6). Performance and use of individual resources was assessed on the basis of reports from simulation (Fig. 7). Subsequently, line retool times were estimated and their impact on performance and organization of work on the line (Fig. 8).

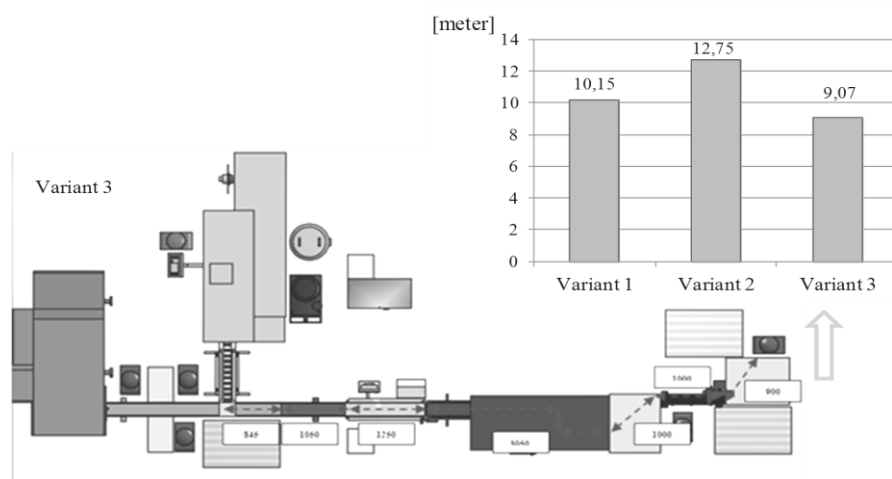


Fig. 6. Distance covered by a product on a line

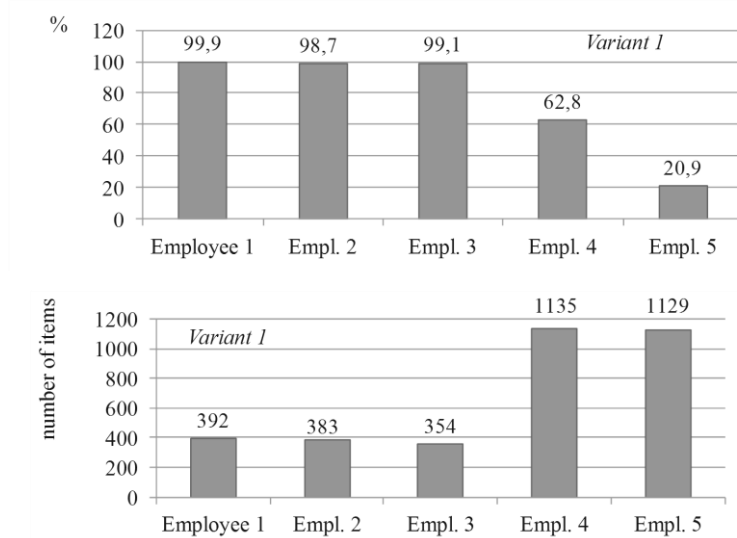


Fig. 7. Performance and use of individual resources: for variant 1

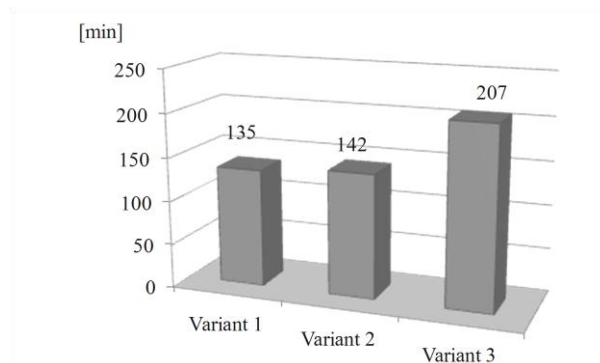


Fig. 8. Line retool time

Variants of solutions were assessed in terms of four criteria, the significance of which was assessed according to the Saaty's method (Fig. 9):

- k_1 : performance,
- k_2 : ergonomics and safety at a work station,
- k_3 : line retool time,
- k_4 : distance covered by a product on a line.

Figure 10 presents number grades of variants for each of the criteria prepared by three decision makers that were brought to normalised grades in the range (0.1).

Next, average grades of variants and indicators for normalised decisions were created, which were obtained by raising components of subsequent normalised grades to a power equal to the appropriate weight (Fig. 11).

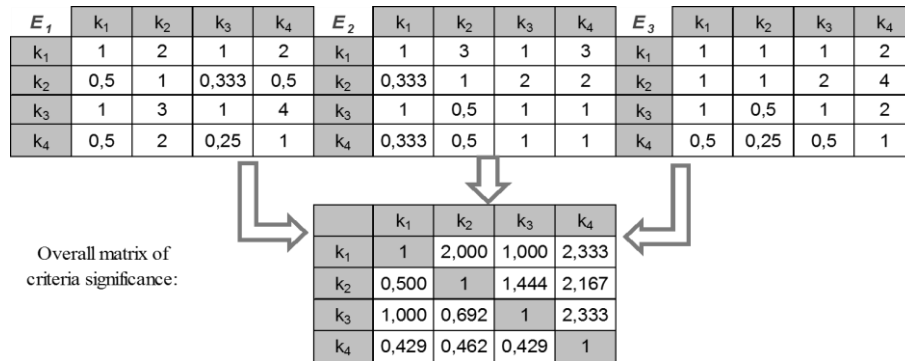


Fig. 9. Criteria significance assessment using the Saaty's method for three experts and an overall matrix of criteria significance

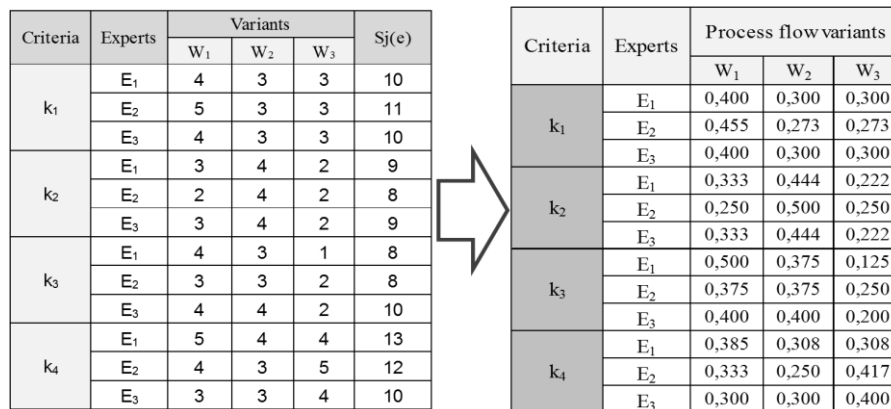


Fig. 10. Bringing number grades of variants to normalised grades

As a result of the presented procedure, the best variant among those indicated in the analysis of the area of acceptable solutions was selected. It turned out to be the solution marked as W_1 .

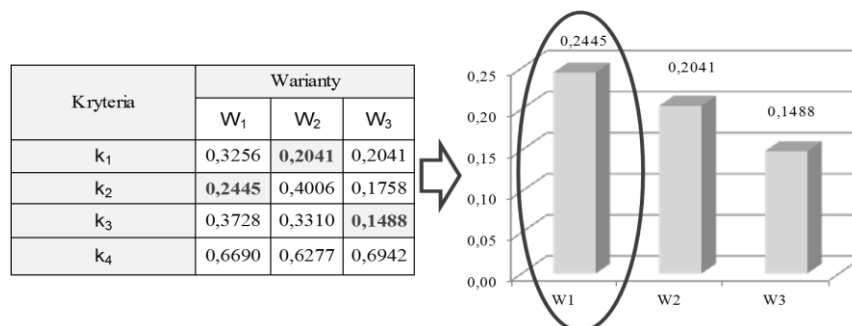


Fig. 11. Bringing number grades of variants to normalised grades

5. CONCLUSIONS

The use of simulation tools requires detailed knowledge of manufacturing process flow and interrelationship of individual cells in an enterprise. Although constructing a model is a time-consuming process, the prepared model can be used for fast verification of various scenarios of solutions relating to functioning of current manufacturing system or manufacturing system being designed.

Generated simulation reports are an important source of information about the analysed system. They enable assessment of system parameters without the need to experiment on a real object.

Thanks to the use of a multi-criteria assessment, it is possible to consider a larger number of criteria, with various significance, by assessing variants verified by a simulation as well as finding a compromise.

Prefer solution is Variant 1 with maximum value in decision function 0.2445.

REFERENCES

- Dennis, P. (2016). *Lean Production simplified*. Boca Raton: CRC Press Taylor & Francis Group.
- Dima, I., Man, M. (2015). *Modelling and simulation in management*. Switzerland: Springer International Publishing.
- Falzon, P. (2015). *Constructive ergonomics*. Boca Raton: CRC Press.
- Kelton, W. D., Sadowski, R. P., & Sturrock, D. T. (2007). *Simulation with ARENA*. New York: McGraw-Hill Inc.
- Kłos, S., Patalas-Maliszewska, J., & Trebuna, P. (2016). Improving manufacturing processes using simulation methods. *Applied Computer Science*, 12(4), 7–17.
- Kukla, S. (2014). Multi-criterion assessment of different variants of casts manufacturing processes. *Archives of Foundry Engineering*, 14(3), 47–50.
- Kukla, S. (2016). Quality and safety assurance of iron casts and manufacturing processes. *Archives of Foundry Engineering*, 16(2), 17–20.
- Maciąg, A., Piertróń, R., & Kukla, S. (2013). *Prognozowanie i symulacja w przedsiębiorstwie*. Warszawa: Polskie Wydawnictwo Ekonomiczne.
- Manas, J. (2015). *The resource management and capacity planning handbook*. USA: McGraw-Hill Companies.
- Pisz, I., Sęk, T., & Zielecki, W. (2013). *Logistyka w przedsiębiorstwie*. Warszawa: Polskie Wydawnictwo Ekonomiczne.
- Plinta, D. (2015). *Modelowanie i symulacja procesów produkcyjnych*. Bielsko-Biała: Wydawnictwo Naukowe Akademii Techniczno-Humanistycznej.
- Rainey, L. B., Tolk, A. (2015). *Modeling and simulation support for system of systems engineering applications*. New Jersey: John Wiley & Sons.
- Rossetti, M. D. (2016). *Simulation modelling and Arena*. New Jersey: John Wiley & Sons.
- Sobaszek, Ł., & Gola, A. (2015). Computer-aided production task scheduling. *Applied Computer Science*, 11(4), 58–69.

*heat transfer, thermal technical chambers, physical modeling,
control process*

Marian JANCZAREK, Oleksij BULYANDRA***

COMPUTER AIDED THERMAL PROCESSES IN TECHNICAL SPACES

Abstract

This paper describes research work on methods concerning heat transfers through walls of thermal technical chambers. The paper presents the mathematical and physical analysis of problems in the field of energy savings and material selection in thermal chambers in controlled gaseous environment. The purpose for the research is to point out areas subjected to the highest energy losses caused by building's construction and geographical orientation of walls in the aspect of daily atmospheric temperature changes emerging on chamber exterior. Thermal problems were solved using computer aided support. The paper presents exemplary measurement results taken in Lublin region during various periods throughout a year.

1. INTRODUCTION

The main purpose for thermal technical storages in central European climate is to provide products of high consumption quality during autumn, winter and spring. Financial inputs connected with the maintenance of the storage are obviously related with the final cost of apple or any other fruit. It is necessary to prolong storage period energetically efficiently to maintain affordable price of apple. Contemporary technological processes make possible to inhibit biochemical and physiological processes that lead to ripening or overripe fruit.

*Institute of Technological Systems of Information, Faculty of Mechanical Engineering, Lublin University of Technology, Nadbystrzycka St. 36, 20-618 Lublin, Poland, m.janczarek@pollub.pl

** National University of Food Technologies, Volodymyrska St, 68, Kiev, Ukraina, 01033, phone: 00380442879453, info@nuft.edu.ua

The prolongation of storage period is mainly achieved by the storage of apple of pear in chambers that can maintain low temperature of fruit, i.e.: within the range between $0 \div +1.5^{\circ}\text{C}$. Beside temperature conditions, it is necessary to provide the air of low oxygen and carbon dioxide contents and of high humidity and circulation in the interior of the cooling chamber. The differences among particular cases of thermal energy demand for storage depends mainly on different construction of cooling chambers. The construction can differ in materials and dimensions which results in different thermal resistance of external walls (Janczarek&Świć; 2012;). Problems of thermal conductivity can be analyzed by many methods, for example: Laplace transformations method, Fourier trans-forms, etc. The paper presents two models: analog one and differential one. They can help to control heat processes during storage periods.

It has to be noted that building design processes require fluent acquaintance of rules and processes described by building physics also in the aspects of thermal preservation. Buildings should meet requirement related energy savings at simultaneous maintenance of thermal comfort in rooms. Some ignorance of thermal processes occurring in such objects, in particular – insufficient thermal conductivity levels in walls can lead to exaggerated energy losses (Bzowska, 2002). This is particularly important because of continuously raising price and increasing pollution of the atmosphere. The parameter that describes wall thermal conductivity is the coefficient of thermal conductivity $\lambda[\text{Wm}^{-1}\text{K}^{-1}]$ (k – in some international reference), which is dependent among others on volume density and material structure, water content and temperature. The coefficient of thermal conductivity is the information of energy flux that flows through a unit area of a material layer of 1 m thickness at the temperature difference at both surfaces of this layer equal to 1 K (1°C). The higher the volume density, the higher is the described coefficient and the material transfers heat more easily. Moreover, the materials composed of the same substance can have different coefficients of thermal conductivity when volume density is different. Thermal conductivity can vary in the function of temperature and the heat loss increases at some proportion together with the temperature difference. This phenomenon is the result of complex changes of heat transfer through: conductance in materials which the layer is composed of, convection in fluid components of porous construction and even through heat radiation on internal and external surfaces of the layer. The more porous material is, it causes the lesser heat transfer and through this it prevents heat from the flow outside the structure (Bzowska, 2000, 2005; Chwieduk, 2006). Practical implementation of this phenomenon was previously described by the author in extremely low or high temperature i.e.: hot tank insulation (Janczarek&Bulyandra, 2016). In building envelope the variation of temperature is comparatively small (except for instance – sun exposed dark surface) and the variation of thermal conductance in dependence on temperature can be omitted. It is, however important to provide information of temperature when λ is determined.

The phenomenon of heat transfer through external walls is one of the most important components of heat loss from buildings. This is either important in buildings of constant occupation or in objects of short time use. Thermal conductance of external walls plays a significant role in these losses. The external walls not only protect the building from thermal losses but also influence interior air quality and its humidity. The building envelope should enable, in some extent, the exchange of air and water vapor at simultaneous humidity stabilization. Moreover, one of the most important physical properties qualifying external wall is its thermal capacity – decisive to building thermal stability in the result of thermal inertia (Dzieniszewski, 2005; Fracastaro, Mutani, & Perino, 2002; Janczarek, 2013). The phenomenon of thermal inertia occurs as a phase shift of heat transfer into the room. Physical properties of wall construction materials undergo disadvantageous changes in the result of dampness which lessens its quality and durability. The efficient protection of building is to avoid negative influence of moisture and to prevent from the following damage. The condition to meet microclimate comfort in rooms is its dry envelope (Lomas, Cook & Fiala, 2007). Damp walls make it impossible even at very intensive heating. Water vapor flow is important in the protection against moisture. Water vapor diffusion through building walls is a process of partial water vapor pressure equalization between two environments divided by the wall. The water vapor flow occurs from the environment of higher concentration to the environment of lower concentration which means that water vapor flows always in the direction of a drier room. The coefficient of vapor transmittance [$\text{mg}/(\text{m}\cdot\text{h}\cdot\text{Pa})$] characterizes material and structure properties related to vapor diffusion. This coefficient describes the content of water vapor expressed in mg that diffuses through 1 m^2 of a material layer of 1 m thickness during 1 hour and at 1 Pa pressure difference on both sides of this layer. Similarly to the heat transfer through the external building envelope, the diffusive resistance of material layers can be determined, i.e.: $Z = d / \delta$, where d is layer thickness [m]. Water enclosed in pores is of λ equal to $0,56 [\text{W}\cdot\text{m}^{-1}\cdot\text{K}^{-1}]$, which is about 20 times the one of air in pore diameter of about 0.05 mm in such material as bricks (Suchorab, 2013). Some additional influence on heat transfer is exerted by water vapor diffusion which increases this transfer and by moisture capillary transport. The moisture content increase is followed by some intensification of thermal conduction and among others, that is why thermal insulation gets worse because water gets inside pores instead of the air (Hunt & Linden, 2001; Voeltzel, Carrie & Guarracino, 2001). This process does not occur identically in different materials and depends on material structure, its origin, e.g. cellular concrete the increase of λ is about 4,5% per 1% moisture content increase.

2. MODELS OF HEAT TRANSFER THROUGH WALL

The purpose of this paper is to describe the design of control systems of cooling and air conditioning systems in storage spaces. For a control systems its necessary to use only three elements: sensor, controller and controlled device. The main of those elements is temperature sensor which shows the picture of thermal decomposition in cold store. The very important are also devices, which provide control of humidity and cyclic potential motion of air in space. It must be noted, that all the control actions depend mainly on measurement of a controlled variable. It is, therefore, necessary to analyze very carefully what is actually being measured, how it may vary with time and which degree of accuracy is necessary in the measurement. Mostly, the temperature of the surfaces on which the sensors are mounted is different from the air temperature (Calvadero&Agnoli, 2007; Kisielewicz, 2003).

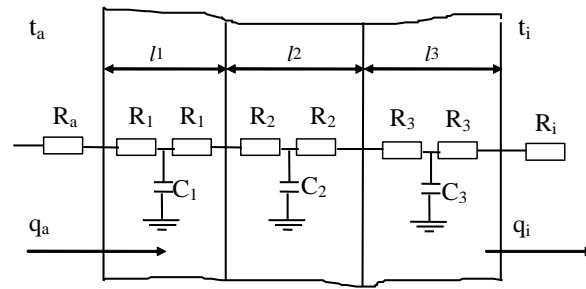


Fig. 1. Model of wall composed of three layers in electrical analogy

Conduction take place when a temperature gradient exists in a solid (or stationary fluid) medium. Energy is transferred from the more energetic to the less energetic molecules when neighboring molecules collide. Conductive heat flow occur in the direction of decreasing temperature because higher temperature is associated with higher molecular energy (Etheridge, 2002). The equation used to express heat transfer by conduction is known as Fourier's Law. The article presents the physical model of heat transfer through chamber walls by means of a mathematical model suitable for sine waveform of internal temperature changes.

From it we can get matrix notation (eventually for n – layers of wall) and the final result of this calculation is a pair of linear relations between the temperature and fluxes at the two surfaces of the composite slabs.

$$[\Delta t_i(p), \Delta q_i(p)] = [\Delta t_a(p), \Delta q_a(p)] \begin{bmatrix} 1 & 0 \\ -R_1 & 1 \end{bmatrix} \begin{bmatrix} 1 & -pC_1 \\ 0 & 1 \end{bmatrix} \cdots \begin{bmatrix} 1 & -pC_n \\ 0 & 1 \end{bmatrix} \begin{bmatrix} 1 & 0 \\ -R_{n+1} & 1 \end{bmatrix} \quad (1)$$

The relation is precisely analogous to Ohm's law for the steady flow of electric current: the flux corresponds to the electric current, and the drop of temperature to the drop of potential. Thus R may be called the thermal resistance of the slab. Next suppose we have a composite wall composed of n slabs of different thickness and conductivities. If the slabs are in perfect thermal contact at their surfaces of separation, the fall of temperature over the whole wall will be the sum of the falls over the component slabs and since the flux is the same at every point, this sum is evidently.

This is equivalent to the statement that the thermal resistance of a composite wall is the sum of the thermal resistance's of the separate layers, assuming perfect thermal contact between them. Finally, consider a composite wall as before, but with contact resistances between the layers such that the flux of heat between the surfaces of consecutive layers is H times the temperature difference between these surfaces. The differential equation to be solved is Fourier's equation.

3. THERMAL RESEARCH ON REAL OBJECT

The verification of the accepted methodology and results have been performed on the data thermal flux density obtained from rural thermal chamber in Radzyń Podlaski (Poland). The small sensor of low inertia has been developed especially for the purpose of the research. This sensor has been used to measure the heat flux density. The experimental analysis proves the necessity to consider the dynamic character of internal temperature when thermal chamber analysis is performed. The thesis includes also the presentation of elaborated methodology of analysis of industrial long term storage.

The purpose for the research is to point out areas subjected to the highest energy loss caused by building construction and geographical orientation of walls. Thermal detectors have been installed on external surfaces, internal surfaces and inside wall layers to measure temperature. The graphical presentation of temperature field distribution on wall surfaces have been performed by means of a thermal vision camera (Fig.3., 4). The camera enables to distinguish visually the areas of the highest thermal loss from storages. The analysis of temperature distribution on vertical walls of storages makes possible to indicate proper building construction of objects. The analysis results are presented in figures. Moreover, temperature measurements taken on chamber external surfaces let us distinguish rooms that serve for other purpose than storage, e.g. a technical room. This room additionally protects the storage from disadvantageous influence of atmospheric conditions.

Article includes analysis of changeable influence in time of variable weather temperature on internal temperature of construction object depending on thermal inertia of building. Taken advantage influence of sinusoidal change external temperature on internal temperature of thermal technical spaces of thermo stability object will allow to get drop of cost of expendable energy of construction object on keeping of definite thermal condition in accommodation properly spaces. It shows harmonist of exemplary characteristic depending on length of time of measurement course of temperature and seasons of the year.

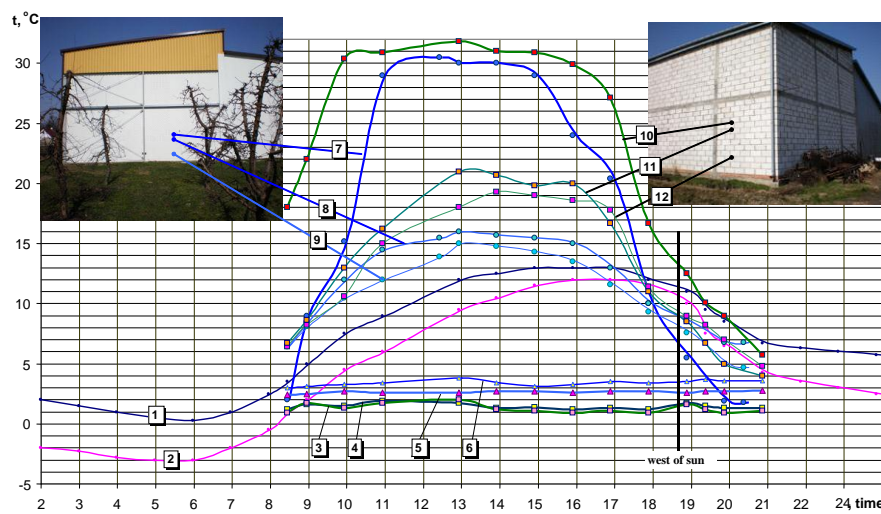


Fig. 2. Presentation of temperature field distribution on wall surfaces

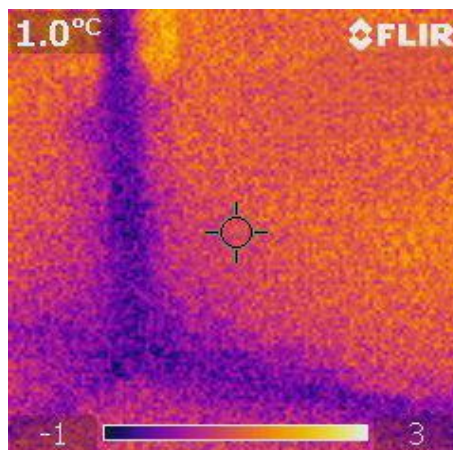


Fig. 3. Temperature field distribution on the corner of wall

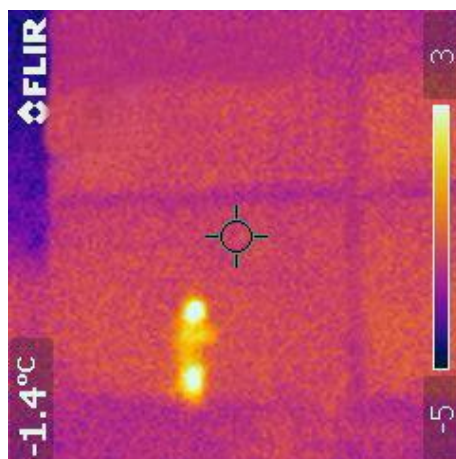


Fig. 4. Temperature field distribution on wall surfaces

4. MEASUREMENT POSITION FOR THE RESEARCHING COEFFICIENT OF HEAT TRANSFER IN MATERIALS

In aim of determined of coefficient of heat transfer of bricks in dependences upon of degree her moistures one chose method experimental. Research one passed on laboratory – position in Technical University of Lublin and referred of measurement of temperatures, thickness of streams warm and moistures relative bricks. As material to driven researches used brick full red both wet and then this oneself brick dried in stove. In time of a few days' measurements driven former at a help of computer registration of temperatures in four points on external surfaces examined bricks as also in two central points in interior. Simultaneously driven former computer registration of moisture at help of two searchers of type WHT installed in center of brick. Values of thickness led of warm density became measured at help of electronic sensors of type PTP, which connected former to universal measure APPA.

Position laboratory – to qualifications of coefficient of heat flow in aspect different moistures of equipped brick was in two chambers. Different conditions thermal in chambers held former at help of aggregates cooling and of controlled warmers. Among chambers one installed investigative sample in typical form full red bricks placed tight to capacity in plate of polystyrene about thickness 20 cm. Polystyrene. Plate used former in aim of isolating of surface external bricks from influence undesirable temperatures. Surfaces external bricks surrendered became {remained} to activity from one side of chamber to temperature $+25^{\circ}\text{C}$ and from second side of chamber to temperature $+1.5^{\circ}\text{C}$. Values these of temperatures registered former independently for every from six sensors, and then recorded on disc of computer at measuring – step carrying out 15 of minutes.

Simultaneously with measurement of temperature registered former at help of programmed computer values of moisture of brick on two separate files. Obtained from measurements of value of temperatures, of streams and moistures became placed in programmer EXCEL. At the help of suitable mathematical transformations coded values of temperatures and moistures exchanged on suitable individuals on degrees °C and on per cent definite values of relative moisture.

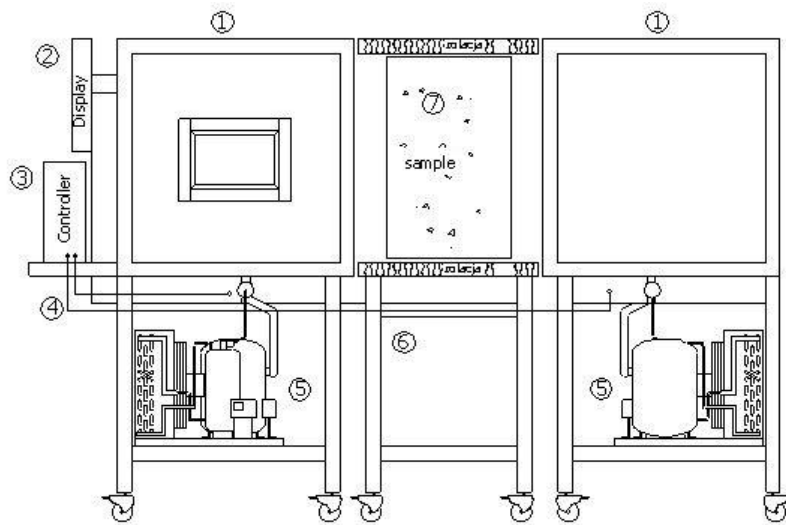


Fig. 5. Schema ideological positions laboratory – to measurement of coefficient of heat transfer.

1. Chamber measuring – executed from aluminum – profiles. Thickness of side 10 cm, with full mineral.
2. Display – LCD Samsung SyncMaster about diagonal 15".
3. Driver – computer PC class with operating – system UNIX.
4. Wires driver steering of generative of microclimate in chambers.
5. Laboratory set of Danfoss firm to generating conditions thermal prevalent inside of chambers. Range of temperatures from -40°C to $+50^{\circ}\text{C}$.
6. Table made from aluminum – profiles with variable construction making possible securing and arrangement of prepared samples to investigations.
7. Primary standard sample of builder's material – full red bricks – placed in polystyrene plate.



Fig. 6. View general positions laboratory – measuring – chambers



Fig. 7. Registering positions laboratory

Correlations among obtained values of coefficient of heat conduction permit on determination of characterizations of graphic coefficient for chance dry and wet bricks.

Obtained results of measurements permitted on qualification of dependence of coefficient of heat transfer from internal temperatures in full red brick wet and dry.

Example – course of changes of value of coefficient of heat transfer. Simultaneously obtained results of value of coefficient of heat transfer permitted on determination of coefficient lambda. From represented below graphs results difference among courses for wet and dry bricks.

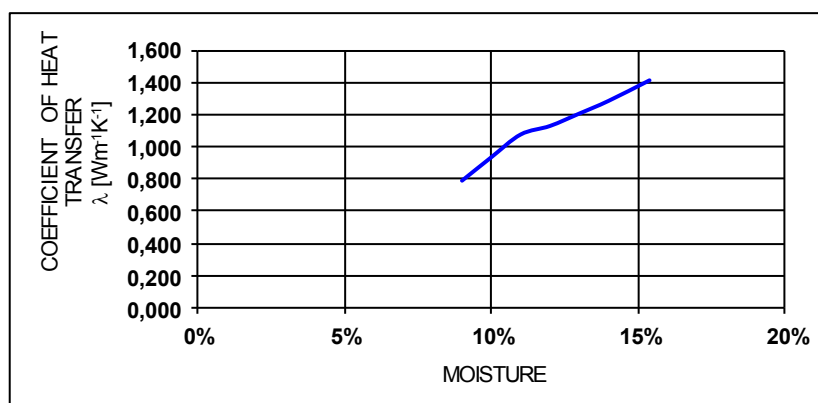


Fig. 8. Characterizations of changes of coefficient of heat transfer in wet full brick

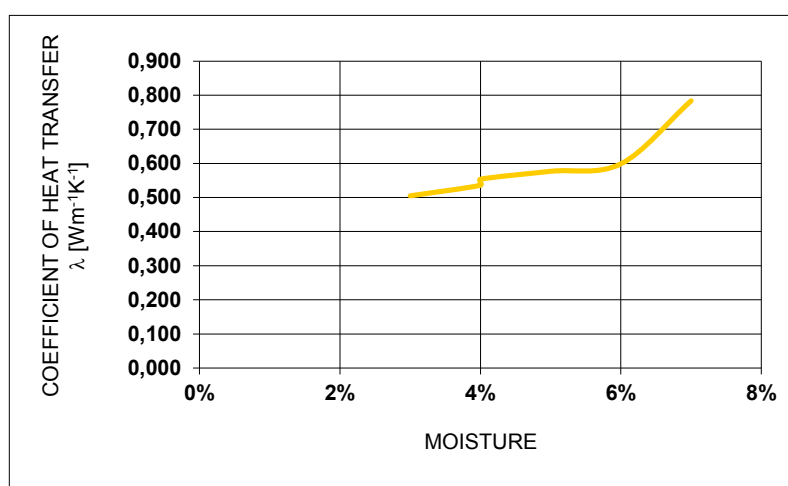


Fig. 9. Characterizations of changes of coefficient of heat transfer in dry full brick

5. CONCLUSION

By the suitable construction of the enclosure walls composed of several slabs of different thicknesses and conductivities, we can obtain phase shift (when the time lag attains twelve hours it is the best situation), which reduce the amplitude of internal temperature inside technical chamber and, in consequence, give equivalent of using energy. The influence of this periodically changing weather temperature upon the inside storages climate is depending on the material of walls and inertial property of thermal technical spaces, it means a fruit storage.

This analysis shows the periodic variability of outside temperature, changing in periods of each day and also in the year with maximum value in the afternoon or in summer and minimum value in the night or winter time. The influence of this periodically changing temperature on the inside storages climate is depending on thermal inertia of technical spaces. The proper construction of an object with prescribed thermo-stability characteristic can use the phase difference between internal and external temperature and allow to lower costs of energy, necessary for cooling or heating the technical spaces.

REFERENCES

- Bzowska, D. (2000). Heating load demand for a room under weather conditions. *Archives of Thermodynamics*, 21(1–2), 43–52.
- Bzowska, D. (2002). Prediction of natural ventilation rates induced by weather parameters. *Archives of Civil Engineering*, 48(4), 473–492.
- Bzowska, D. (2005). Natural ventilation induced by weather parameters in two-zone building. *Archives of Civil Engineering*, 51(1), 135–151.
- Calderaro, V., & Agnoli, S. (2007). Passive heating and cooling strategies in an approaches of retrofit in Rome. *Energy and Buildings*, 39(8), 875–885. doi:10.1016/j.enbuild.2006.10.008
- Chwieduk, D. (2006). Modelowanie i analiza pozyskiwania oraz konwersji termicznej energii promieniowania słonecznego w budynku. *Prace Instytutu Podstawowych Problemów Techniki PAN*, 11, 5–262.
- Dzieniański, W. (2005). *Procesy ciepłno-przepływowe w budynkach: podstawy modelowania matematycznego*. Łódź: Komitet Inżynierii Łądowej Wodnej PAN.
- Etheridge, D. (2002). Nondimensional methods for natural ventilation design. *Building and Environment*, 37(11), 1057–1072. doi:10.1016/S0360-1323(01)00091-9
- Fracastaro, G., Mutani, G., & Perino, M. (2002). Experimental and theoretical analysis of natural ventilation by window openings. *Energy and Buildings*, 34(8), 817–827. doi:10.1016/S0378-7788(02)00099-3
- Hunt, G. R., & Linden, P. F. (2001). Steady-state flows in an enclosure ventilated by buoyancy forces assisted by winds. *Journal of Fluid Mechanics*, 426, 355–386.
- Janczarek, M. M. (2013). Analiza matematyczno-fizyczna ciepłych komór technicznych. In M. Janczarek & J. Lipski (Eds.), *Technologie informacyjne w technice i kształceniu* (pp. 127–137). Lublin: Politechnika Lubelska.
- Janczarek, M. M., & Świć, A. (2012). Scientific and technological description of heat and mass transfer processes in chambers. *Annals Of Faculty Of Engineering Hunedoara–International Journal Of Engineering*, 10, 55–60.

- Janczarek, M., & Bulyandra, O. (2016). Computer modeling of energy saving effects. *Applied Computer Science*, 12(3), 47–60.
- Kisilewicz, T. (2003). *Stateczność cieplna budynków pasywnych*. Paper presented at the IX Polska Konferencja Naukowo-Techniczna Fizyka Budowli w Teorii i Praktyce, Łódź, Poland.
- Lomas, K., Cook, M., & Fiala, D. (2007). Low energy architecture for severe US climate: Design and evaluation on a hybrid ventilation strategy. *Energy and Buildings*, 39(1), 32–44. doi: 10.1016/j.enbuild.2006.03.032
- Suchorab, Z., Sobczuk, H., & Lagod, G. (2016). Estimation of Building Material Moisture Using Non-invasive TDR Sensors. In L. Pawłowski (Ed.), *Environmental Engineering IV* (pp.433–439). London: Taylor & Francis Group. doi:10.1201/b14894-64
- Voeltzel, A., Carrie, F. R., & Guarracino, G. (2001). Thermal and ventilation modelling of large highly-glazed spaces. *Building and Environment*, 33(2), 121–132. doi: 10.1016/S0378-7788(00)00074-8